Molecular Plant Advance Access published July 17, 2013

Heteromeric and Homomeric Geranyl Diphosphate Synthases from *Catharanthus roseus* and Their Role in Monoterpene Indole Alkaloid Biosynthesis

Avanish Rai[a], Shachi S. Smita[b], Anup Kumar Singh[a], Karuna Shanker[b] and **Dinesh A. Nagegowda[a,1]**

a CSIR–Central Institute of Medicinal and Aromatic Plants Research Centre, Bangalore, 560065, India
b CSIR–Central Institute of Medicinal and Aromatic Plants, Lucknow, 226015, India

ABSTRACT ***Catharanthus roseus*** **is the sole source of two most important monoterpene indole alkaloid (MIA) anti-cancer agents: vinblastine and vincristine. MIAs possess a terpene and an indole moiety derived from terpenoid and shikimate pathways, respectively. Geranyl diphosphate (GPP), the entry point to the formation of terpene moiety, is a product of the condensation of isopentenyl diphosphate (IPP) and dimethylallyl diphosphate (DMAPP) by GPP synthase (GPPS). Here, we report three genes encoding proteins with sequence similarity to large subunit (CrGPPS.LSU) and small subunit (CrGPPS.SSU) of heteromeric GPPSs, and a homomeric GPPSs. CrGPPS.LSU is a bifunctional enzyme producing both GPP and geranyl geranyl diphosphate (GGPP), CrGPPS.SSU is inactive, whereas CrGPPS is a homomeric enzyme forming GPP. Co-expression of both subunits in *Escherichia coli* resulted in heteromeric enzyme with enhanced activity producing only GPP. While *CrGPPS.LSU* and *CrGPPS* showed higher expression in older and younger leaves, respectively, *CrGPPS.SSU* showed an increasing trend and decreased gradually. Methyl jasmonate (MeJA) treatment of leaves significantly induced the expression of only *CrGPPS.SSU.* GFP localization indicated that CrGPPS.SSU is plastidial whereas CrGPPS is mitochondrial. Transient overexpression of *AmGPPS.SSU* in *C. roseus* leaves resulted in increased vindoline, immediate monomeric precursor of vinblastine and vincristine. Although *C. roseus* has both heteromeric and homomeric GPPS enzymes, our results implicate the involvement of only heteromeric GPPS with CrGPPS.SSU regulating the GPP flux for MIA biosynthesis.**

Key words: ***C. roseus*****; monoterpene indole alkaloids; geranyl diphosphate synthase; heteromer; homomer; large subunit; small subunit; vindoline.**

INTRODUCTION

Plants produce a vast array of natural products also called secondary metabolites as a means of self-defense against herbivores and pathogens. Alkaloids are one such class of compounds produced by about 20% of plant species and are mostly derived from amino acids. Monoterpene indole alkaloids (MIAs) represent one of the largest classes of alkaloids consisting of ~3000 different compounds, some of which have been shown to possess powerful pharmacological activities (Facchini and De Luca, 2008). The MIAs have been reported to be present in eight different plant families, but are most commonly found in Apocyanaceae, Loganiaceae, and Rubiaceae families (Facchini and De Luca, 2008). Madagaskar Periwinkle (*C. roseus*) belonging to Apocyanaceae family is a medicinal plant of enormous importance, as it produces more than 130 MIAs (van der Heijden et al., 2004) and it is the only source of two most important anti-cancer dimeric MIAs—vinblastine and vincristine—and one of their monomeric precursors—vindoline (Liscombe and O'Connor, 2011). The dimeric MIAs vinblastine and vincristine, which accumulate in *C. roseus* leaves at very low amounts (0.0003–0.01%), are condensation products of vindoline and catharanthine monomers (Liscombe and O'Connor, 2011). Approximately 35 intermediates and more than 30 enzymes are responsible for the biosynthesis of bisindole alkaloids involving different

[1] To whom correspondence should be addressed. E-mail da.nagegowda@cimap.res.in, tel. 91–080–28460565, fax 91–080–28564707.

doi: 10.1093/mp/sst058

Received 12 November 2012; accepted 20 March 2013

subcellular compartments and require exclusive transport of pathway intermediates (St-Pierre et al., 1999; van der Heijden et al., 2004). The complex multi-step MIA biosynthetic pathway is under strict regulation of developmental, environmental, organo-, and cell-specific controls (Aerts et al., 1994; Vázquez-Flota and De Luca, 1998; St-Pierre et al., 1999; van der Heijden et al., 2004; Rischer et al., 2006; Wei, 2010). The biosynthesis of strictosidine, which serves as the central precursor for all downstream steps leading to MIAs, involves condensation of shikimate pathway-derived indole moiety, tryptamine, and terpene pathway-derived moiety, secologanin (Facchini and De Luca, 2008) (Figure 1). Precursor feeding experiments have shown that the formation of monoterpene moiety is rate-limiting in MIA biosynthesis (Arvy et al., 1994; Hedhili et al., 2007). Geranyl diphosphate (GPP), the universal precursor for all monoterpenes (Dudareva et al., 2006), is the entry point for the formation of secologanin (Figure 1). GPP is formed by the condensation of dimethylallyl diphosphate (DMAPP) and isopentenyl diphosphate (IPP) in a reaction catalyzed by GPP synthase (GPPS, EC 2.5.1.1) (Ogura and Koyama, 1998), which belongs to the family of short-chain prenyltransferases (Figure 1). GPP is subsequently converted to geraniol, 10-hydroxygeraniol, loganin, and ultimately to secologanin via multiple enzymatic steps (Liu et al., 2007). The short-chain prenyltransferases also include farnesyl diphosphate (FPP) synthase (FPPS; EC 2.5.1.10) and GGPP synthase (GGPPS; EC 2.5.1.30) (Tholl et al., 2004). All these short-chain prenyltransferases function at the branch points of isoprenoid metabolism and play regulatory role in controlling IPP flux into various terpenoid families (Gershenzon and Croteau, 1993; Liang et al., 2002).

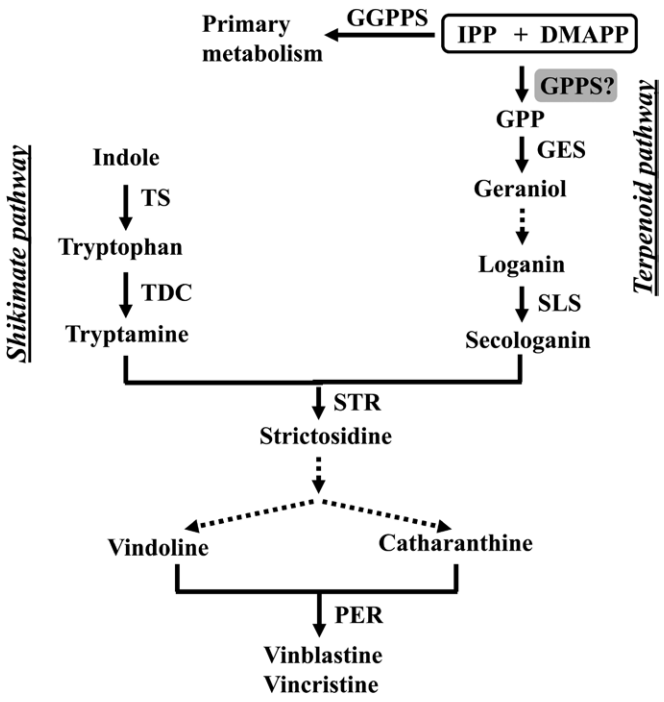

Figure 1. Simplified View of MIA Biosynthesis in *C. roseus.*
Full and dashed arrows indicate single and multiple enzymatic steps, respectively. The key branch-point step by geranyl diphosphate synthase (GPPS) has been highlighted. DMAPP, dimethylallyl diphosphate; GES, geraniol synthase; GGPP, geranylgeranyl diphosphate; GGPPS, GGPP synthase; GPP, geranyl diphosphate; IPP, isopentenyl diphosphate; PER, peroxidase; SLS, secologanin synthase; STR, strictosidine synthase; TDC, tryptophan decarboxylase; TS, tryptophan synthase.

GPPSs have been characterized in few plant species and exist as homomeric and heteromeric structures (Nagegowda, 2010). The homomeric GPPSs are reported in two gymnosperm species (*Abies grandis* and *Picea abies*) (Burke and Croteau, 2002a, 2002b; Schmidt and Gershenzon, 2007, 2008; Schmidt et al., 2010) and four angiosperm species (*Arabidopsis thaliana*, *Lycopersicon esculentum*, *Quercus robur*, and *Phalaenopsis bellina*) (Bouvier et al., 2000; van Schie et al., 2007; Hsiao et al., 2008; Schmidt and Gershenzon, 2008). The heteromeric GPPSs have been reported only in angiosperms that include *Mentha piperita*, *Antirrhinum majus*, *Clarkia breweri*, and *Humulus lupulus*, all of which produce large amounts of monoterpenes in specific organs such as trichomes and flower petals (Burke et al., 1999; Tholl et al., 2004; Wang and Dixon, 2009). Structurally, the heteromeric GPPS is composed of a non-catalytic small subunit (SSU) and a large subunit (LSU), which could be either inactive (Burke et al., 1999) or function as GGPPS on its own (Tholl et al., 2004; Wang and Dixon, 2009), and interaction between the two subunits results in an active heteromeric GPPS. So far, little is known about the type of GPPS present in MIA biosynthesizing plants despite the fact that this enzyme catalyzes the branch-point reaction leading to GPP, which serves as substrate for the monoterpene moiety of all MIAs. It has been reported that homomeric GPPS in gymnosperms and SSUs of heteromeric GPPS regulate monoterpene biosynthesis (Tholl et al., 2004; Hsiao et al., 2008; Wang and Dixon, 2009; Schmidt et al., 2010). Moreover, in tobacco, the endogenous pool of GPP was shown to be limiting for monoterpene biosynthesis (Orlova et al., 2009). In *C. roseus* also, GPPS may play a regulatory role in controlling the flux towards formation of MIAs. Hence, it is important to know the type(s) and the role of GPPS in MIA biosynthesis for eventual metabolic engineering for improved accumulation of MIAs.

In this work, we report functional characterization of heteromeric and homomeric GPPSs from *C. roseus*. We show that CrGPPS.LSU by itself is a bifunctional G(G)PPS producing both GPP and GGPP, and, in combination with CrGPPS. SSU, it functions as LSU forming only GPP, whereas CrGPPS falls into homomeric GPPS class and produces GPP as the sole product. The biochemical characterization and MeJA elicitation studies, and analysis of subcellular localization indicated the involvement of CrGPPS.SSU in regulating the flux for MIA biosynthesis, whereas the other two CrGPPS.LSU and CrGPPS could be involved in the formation of plastidial GPP/GGPP for monoterpene biosynthesis and mitochondrial GPP for other

isoprenoid biosynthesis, respectively. This is the first report of characterization of both heteromeric and homomeric GPPS enzymes from the same plant.

RESULTS AND DISCUSSION

Isolation of *C. roseus* cDNAs Encoding GPP Synthases

In plants, the enzyme responsible for GPP formation is known to exist either as homomeric or as heteromeric forms (Burke et al., 1999; Bouvier et al., 2000; Burke and Croteau, 2002a, 2002b; Tholl et al., 2004; Schmidt and Gershenzon, 2007; van Schie et al., 2007; Schmidt and Gershenzon, 2008; Orlova et al., 2009; Chang et al., 2010). To identify and investigate the role of GPPS in *C. roseus* MIA biosynthesis, a search for potential GPPS sequences was carried out initially by blast search analysis against the NCBI (www.ncbi.nlm.nih.gov/) database and later against the recently released MPGR (http://medicinalplantgenomics.msu.edu) database. A search for potential gene encoding GPPS.LSU yielded four potential GGPPSs. The first sequence, named CrGGPPS1 (for *C. roseus* GGPPS), is represented by a sequence submitted in GenBank (GGPPS; JF896104) and two contigs annotated as *GGPPS* in MPGR (cra_locus_1452_iso_1_len_1087_ver_3 and cra_locus_1452_iso_2_len_1656_ver_3). This gene has been recently shown by genetic complementation as a functional GGPPS (Thabet et al., 2012). The second sequence referred to as CrGGPPS2 is represented by three contigs (cra_locus_6993_iso_3_len_1491_ver_3, cra_locus_6993_iso_2_len_1416_ver_3, and cra_locus_6993_iso_1_len_1405_ver_3) with an annotation as GGPPS. The third and the fourth sequences, named *CrGGPPS3* and *CrGGPPS4*, are represented by single contigs cra_locus_6454_iso_5_len_849_ver_3 and cra_locus_12153_iso_7_len_1107_ver_3, respectively. Of these *CrGGPPS1*, *CrGGPPS2*, and *CrGGPPS4* encoded full-length open reading frames, whereas *CrGGPPS3* was missing the 3′ region, which was obtained by rapid amplification of cDNA ends (RACE). The ORFs with 1656 bp, 1491 bp, 1144 bp, and 1107 bp of *CrGGPPS1*-, *CrGGPPS2*-, *CrGGPPS3*-, and *CrGPPS4*-encoded proteins of 383 aa (M_r, 41 599), 371 aa (M_r, 40 156), 306 aa (M_r, 33 141), and 343 aa (M_r, 37 645), respectively. A BLASTP analysis of CrGGPPSs against the NCBI database (www.ncbi.nlm.nih.gov/) revealed that CrGGPPS1, CrGGPPS2, CrGGPPS3, and CrGGPPS4 showed highest amino acid sequence similarity to the LSU from *A. majus* (Tholl et al., 2004), GGPPSs from *Nicotiana tabacum* (Orlova et al., 2009), *Hevea brasiliensis* (Takaya et al., 2003), *Corylus avellana* (Wang et al., 2010), respectively. Further, pairwise sequence percent identity of CrGGPPSs and other plant GGPPSs/LSUs (Table 1) revealed that, among four CrGGPPSs, CrGGPPS1 showed the highest sequence identity of (70–74%) to LSUs of heteromeric GPPSs from *A. majus* (Tholl et al., 2004), *H. lupulus* (Wang and Dixon, 2009), and *M. piperita* (Burke et al., 1999) (Figure 2A). Further, MPGR blast search with known SSU-I and SSU-II sequences yielded a partial length sequence (referred to as *CrGPPS.SSU*) of 763 bp (PUT-165a-Catharanthus_roseus-1810024) corresponding to SSU-I class (Wang and Dixon, 2009). However, a comprehensive search for sequences similar to SSU-II class did not yield any sequences, indicating that *C. roseus* has only SSU-I class. The missing 3′-translated region of *CrGPPS.SSU* was recovered by 3′ RACE. The full-length CrGPPS.SSU encoded a 299-aa (M_r, 32 376) protein. Amino acid sequence comparison exhibited homology of CrGPPS.SSU to other plant GPPS. SSUs and showed 57%, 54%, and 51% identities to SSUs of *A. majus* (Tholl et al., 2004), *M. piperita* (Burke et al., 1999), and *H. lupulus* (Wang and Dixon, 2009), respectively (Figure 2B). This *CrGPPS.SSU* was represented by five contigs in the MPGR database.

A homology search to isolate the homomeric GPPS resulted in a full-length gene sequence submitted in NCBI as GPS (EU622902), which is represented by seven contigs in MPGR. This gene is hereafter referred to as *CrGPPS*. The full-length *CrGPPS* cDNA (1263 bp) encoded a protein of 420 aa (M_r, 46 329). The sequence comparison of CrGPPS exhibited the highest similarity to other characterized angiosperm or gymnosperm homomeric GPPSs with 76% identity to *L. esculentum*, 74% identity to *Q. robur* GPPS (Schmidt and Gershenzon, 2008), and 67% and 65% identities to GPPS from *A. thaliana* (Bouvier et al., 2000; van Schie et al., 2007) and *P. abies* (Schmidt and Gershenzon, 2008), respectively (Figure 3). The alignment of sequences of different homomeric and heteromeric enzymes showed the presence of two highly conserved aspartate-rich regions, designated as the first aspartate-rich motif (FARM, $DDX_{(2-4)}D$) and second aspartate-rich motif (SARM, DDXXD) (where D indicates Asp, X indicates any residue) essential for catalytic function and substrate binding (Koyama et al., 1996; Wang and Ohnuma, 2000) whereas CrGPPS.SSU lacks both $DD(X_n)D$ motifs (Tholl et al., 2004). Further comparisons of sequences highlight the presence of two conserved CxxxC motifs (where 'x' can be alanine, leucine, isoleucine, valine, glycine, or serine) in CrGPPS.SSU similarly

Table 1. Sequence Relatedness of CrGGPPS and Plant GGPPS/LSU Proteins.

	(1)	(2)	(3)	(4)	(5)	(6)	(7)	(8)	(9)	(10)
(1) CrGGPPS1	100									
(2) AmGPPS.LSU	74	100								
(3) HlGPPS.LSU	70	69	100							
(4) MpGPPS.LSU	69	68	69	100						
(5) CrGGPPS2	65	64	68	62	100					
(6) NtGGPPS1	63	57	68	63	74	100				
(7) CrGGPPS4	62	59	60	58	60	57	100			
(8) AtGGPPS6	58	58	60	57	58	56	54	100		
(9) NtGGPPS2	55	57	57	56	57	55	52	52	100	
(10) CrGGPPS3	46	44	42	42	52	39	52	43	39	100

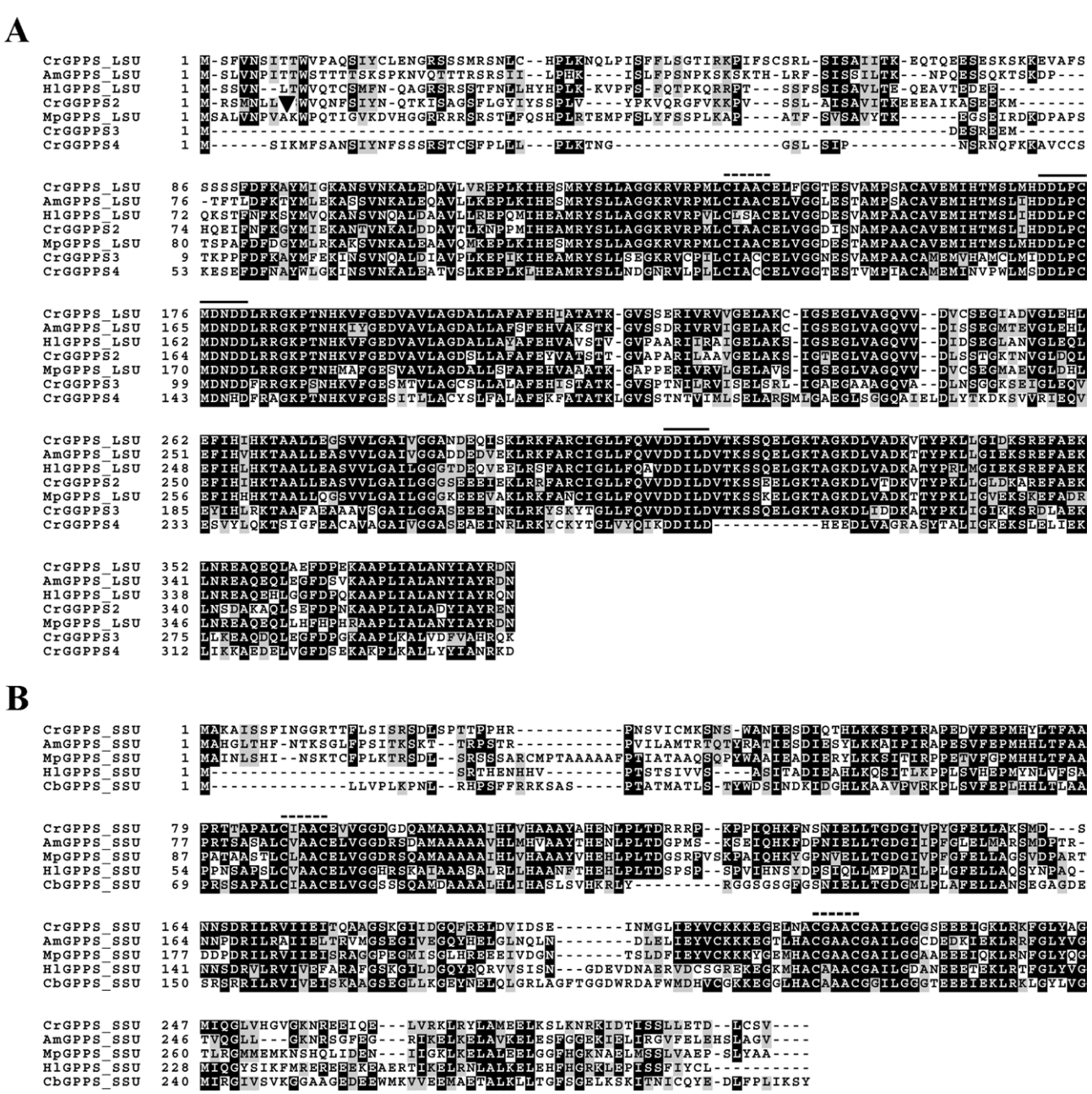

Figure 2. Multiple Sequence Alignment of Plant Heteromeric GPP Synthases.
(A) Amino acid sequence alignment of LSUs from *C. roseus* (CrGPPS.LSU; JX417183), *M. piperita* (MpGPPS.LSU; AF182828), *A. majus* (AmGPPS.LSU; AAS82860), and *H. lupulus* (HlGPPS.LSU; ACQ90682), and CrGGPPSs.
(B) SSUs from *M. piperita* (MpGPPS.SSU; AF182827), *A. majus* (AmGPPS.SSU; AAS82859), *H. lupulus* (HlSSU; ACQ90681), and *C. breweri* (CbGPPS. SSU; AY534745) along with CrGPPS.SSU (JX417184) are included in the alignment. Residues in black are conserved (identical in at least four out of seven in (A) and three out of five in (B), whereas residues in gray are similar in at least two of the sequences shown. Dashes indicate gaps inserted for optimal alignment. The two conserved Asp-rich motifs (FARM and SARM) and CxxxC motifs are indicated by solid line and dotted line, respectively.

to all other SSUs and one such conserved motif in CrGPPS. LSU similarly to other LSUs/GGPPSs. Like other characterized homomeric GPPSs, CrGPPS lacks the CxxxC motif (Figures 2 and 3). The CxxxC motifs are critical for physical interaction between both subunits of plant heterodimeric GPPSs (Wang and Dixon, 2009). Prediction programs like TargetP 1.1, PREDOTAR, ChloroP, and MitoProt indicated the presence of a transit peptide in CrGPPS.LSU and CrGPPS.SSU, suggesting their plastidial localization, and a signal peptide for mitochondrial localization in CrGPPS (Supplemental Table 1).

Heterologous Expression in *Escherichia coli* and Functional Characterization of Heteromeric CrGPPS

In orchid *P. bellina*, an active homodimeric GPPS with similarity to the SSU class of proteins contributes to monoterpene emission. This protein lacks FARM and SARM motifs, but has GPPS activity. CrGPPS.SSU significantly homologous to all other SSUs displays 33% sequence identity to PbGPPS from *P. bellina* (Hsiao et al., 2008). To know whether CrGPPS.SSU has any activity, *CrGPPS.SSU* cDNA with $(His)_6$-tag was expressed and purified (Figure 4D, lane 2). The purified recombinant CrGPPS.SSU had no detectable prenyltransferase activity with IPP and DMAPP (Figure 4E and 4F, panel 2). This inactive nature of SSU is similar to previously reported SSUs from *M. piperita* (Burke et al., 1999), *A. majus*, *C. breweri* (Tholl et al., 2004), *H. Lupulus*, and *A. thaliana* AtSSU-II, which constitutes a distinct clade of *trans*-prenyltransferases and contains first conserved $DDX_{(2-4)}D$ motif and two CxxxC motif but lacks SARM motif (Wang and Dixon, 2009).

It is known that plants contain multiple GGPPS or GGPPS-related enzymes, in which some function as LSU of heteromeric GPPS (Tholl et al., 2004; Orlova et al., 2009; Wang and Dixon, 2009). The isolated sequences clearly suggest the scenario of multiple GGPPS enzymes in *C. roseus* similar to *A. thaliana* (Okada et al., 2000). However, one of these may act as LSU in combination with SSU to form a functional heteromer. Hence, to identify the GPPS.LSU, the open reading frame of CrGPPS.SSU without $(His)_6$-tag was co-expressed individually with CrGGPPSs (lacking transit peptide) carrying a $(His)_6$-tag. Earlier studies with GPPS and GGPPS have shown optimal expression of soluble proteins only after deleting the N-terminal transit-peptide sequence (Burke and Croteau, 2002a). Purification of co-expressed recombinant proteins and their subsequent sodium dodecyl sulfate–polyacrylamide gel electrophoresis (SDS–PAGE) analysis revealed the interaction of only CrGGPPS1 among all CrGGPPSs with CrGPPS.SSU, which is evident from co-purified bands of both subunits (Figure 4A, lane 1). Moreover, the prenyltransferase activity assay with [1-^{3}H]-IPP and DMAPP confirmed the formation of an active heteromeric complex containing CrGGPPS1 and CrGPPS.SSU (Figure 4B). Although all CrGGPPSs possess one CxxxC motif similar to other characterized LSUs that is critical for interaction with SSU, only CrGGPPS1 interacted with CrGPPS.SSU, suggesting that the CxxxC motif is necessary but not sufficient for physical interaction (Wang and Dixon, 2009). It is not surprising that the other three CrGGPPSs did not show interaction with CrGPPS.SSU, as it was also reported in the case of *Arabidopsis* GGPPSs that AtGGPPS6 and AtGGPPS11 possess one CxxxC motif, but only the latter interacted with AtSSU (Wang and Dixon, 2009). Moreover, AtSSU also interacted with *H. lupulus* GPPS.LSU (Wang and Dixon, 2009). The pairwise percentage analysis of deduced amino acid sequences of CrGGPPSs with other LSUs and GGPPSs indicated that only CrGGPPS1 is closely related to LSUs (Table 1). Also, in tobacco, two GGPPS proteins interacted with AmGPPS.SSU (Orlova et al., 2009), indicating that further studies are required to understand

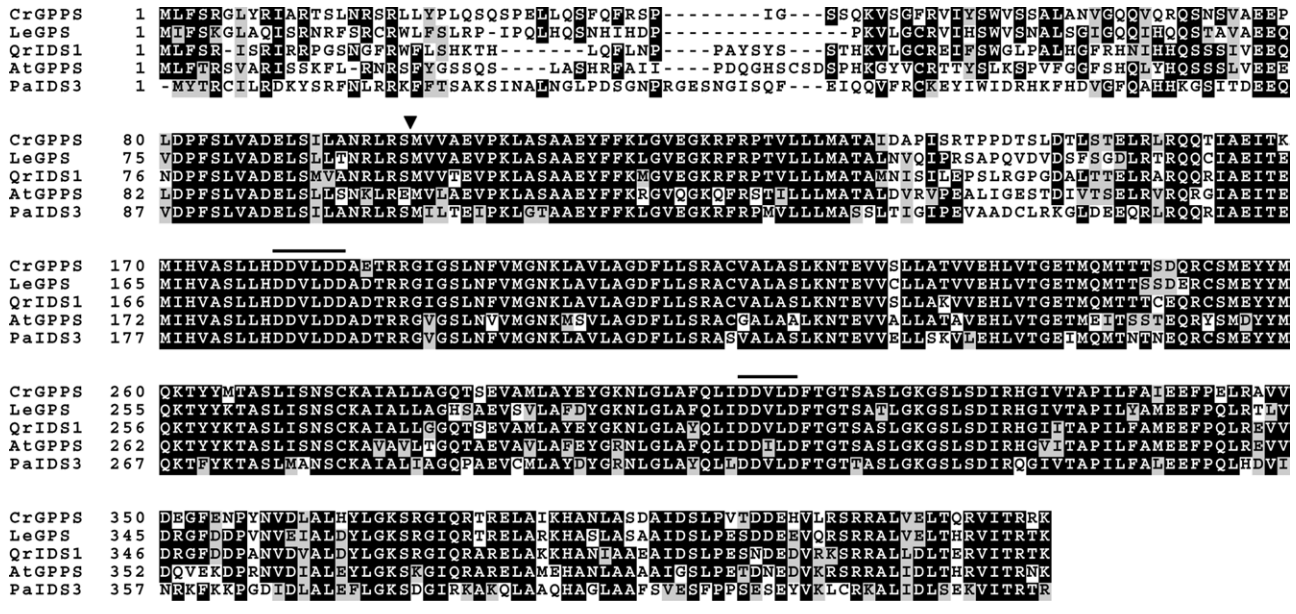

Figure 3. Multiple Sequence Alignment of Plant Homomeric GPP Synthases.
The characterized GPPSs from *L. esculentum* (LeGPS; DQ286930), *A. thaliana* (AtGPPS; Y17376), *P. abies* (PaIDS3; EU432047), and *Q. robur* (QrIDS1; CAC20852) are included in sequence alignment along with *C. roseus* (CrGPPS, JX417185). Conserved residues are in black (identical in at least three out of six sequences shown) and residues in gray are similar in at least two of the six sequences shown. The two conserved Asp-rich motifs (FARM and SARM) are indicated by solid line. The black inverted triangle indicates the truncation site for CrGPPS expressed in *E. coli* as a pseudomature form.

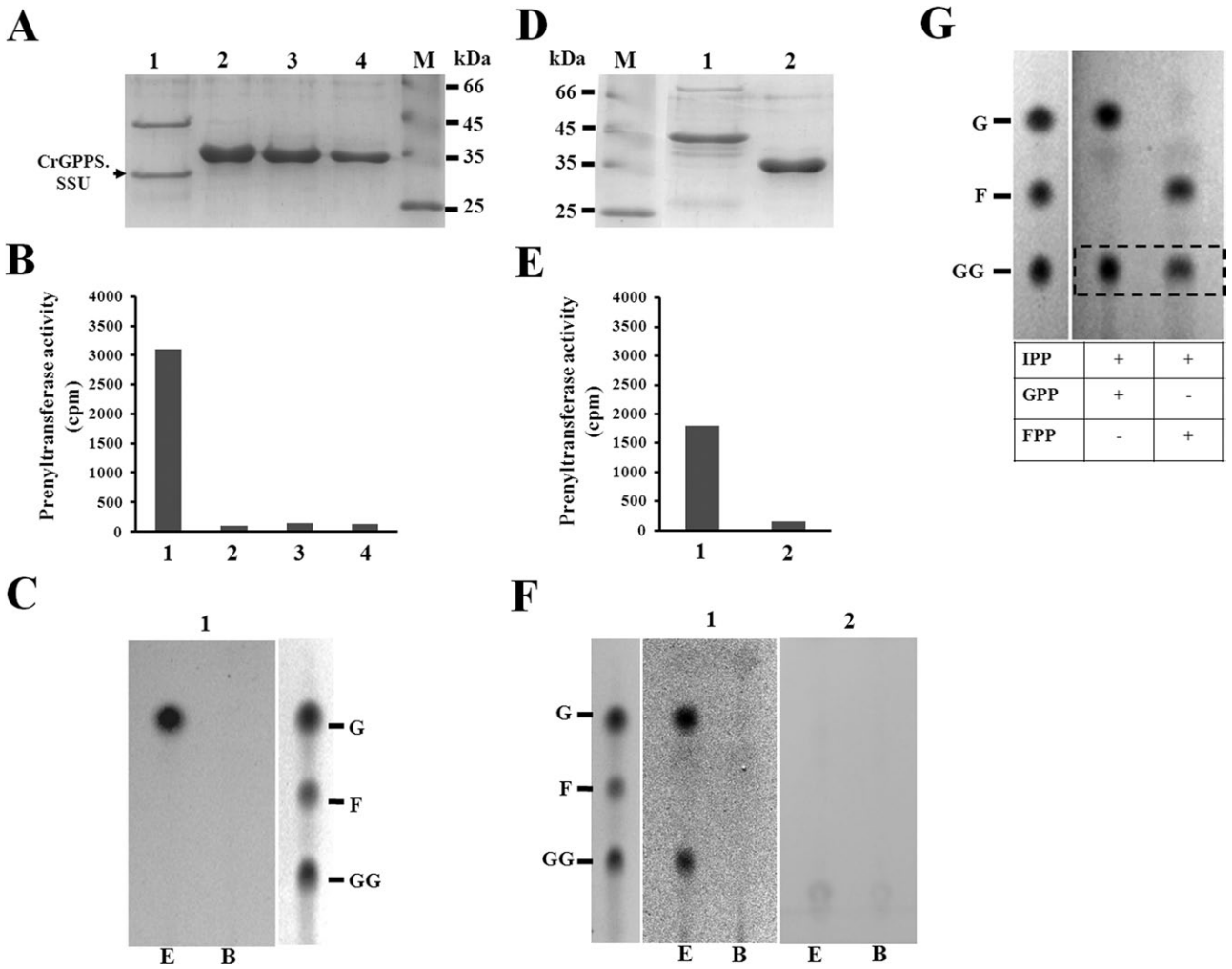

Figure 4. Purification and Prenyltransferase Assay of Recombinant Heteromeric CrGPPS Expressed in *E. coli*.

(A) SDS–PAGE analyses of co-expressed $(His)_6$-tagged CrGGPPSs with non-$(His)_6$-tagged CrGPPS.SSU. Samples contained purified proteins obtained from the co-expression of $(His)_6$–CrGGPPS1 and CrGPPS.SSU (lane 1), $(His)_6$–CrGGPPS2 and CrGPPS.SSU (lane 2), $(His)_6$–CrGGPPS3 and CrGPPS.SSU (lane 3), and $(His)_6$–CrGGPPS4 and CrGPPS.SSU (lane 4). Co-purified CrGPPS.SSU is indicated by an arrow.

(B) *In vitro* prenyltransferase assay of corresponding purified enzymes (as in (A)) in the presence of [1-^{3}H]–IPP and DMAPP.

(C) TLC analysis of products generated by recombinant heteromeric CrGPPS (CrGGPPS1+CrGPPS.SSU) in the presence of IPP and DMAPP.

(D) SDS–PAGE profile of purified CrGPPS.LSU (lane 1) and CrGPPS.SSU (lane 2) and their corresponding prenyltransferase activity with DMAPP and [1-^{3}H]-IPP **(E)**. The cpm values were deducted from the background cpm values of empty vector control reaction.

(F) TLC analysis of products from *in vitro* assays of purified CrGPPS.LSU (1) and CrGPPS.SSU (2), respectively, in the presence of allylic substrates DMAPP and IPP.

(G) TLC analysis of products from *in vitro* assays of purified CrGPPS.LSU in the presence (+) or absence (–) of GPP/FPP with IPP. The product formed is indicated by a dashed box, while other spots are un-reacted substrates. Reaction products were hydrolyzed to their corresponding alcohols, extracted with hexane, and separated by reverse-phase thin layer chromatography. The products were visualized by exposing the TLC plates to iodine vapor and compared with authentic standards G (geranol), F (farnesol), and GG (geranylgeranol). Assays contained recombinant 5–20 µg of purified proteins. E, enzyme; B, boiled enzyme. Boiled protein is used as negative control.

the exact mechanism of LSU and SSU interaction. Since CrGGPPS1 interacted with CrGPPS.SSU, we hereafter refer to this as CrGPPS.LSU.

It has been reported in heteromeric GPPS that LSU alone could be either inactive (Burke et al., 1999) or function as a bona fide GGPPS enzyme on its own (Tholl et al., 2004; Wang and Dixon, 2009). Hence, to identify the function of CrGPPS.LSU, a truncated version starting from second methionine (M-27) was expressed in *E. coli* as a $(His)_6$-tagged protein. The assay with soluble extracts containing recombinant $(His)_6$–CrGPPS.LSU proteins using [1-^{3}H]-IPP and DMAPP as substrates and Mg^{2+} as cofactor detected prenyltransferase activity. This activity was further confirmed using purified $(His)_6$–CrGPPS.LSU proteins (Figure 4D, lane 1, and Figure 4E, panel 1). Product verification of $(His)_6$–CrGPPS.LSU enzyme assay using IPP and DMAPP revealed the formation of both

GPP and GGPP (~2:1) indicating the bifunctional nature of this enzyme (Figure 4F, panel 1). The bifunctional CrGPPS.LSU could provide both GPP and GGPP pool. GPP could be used as a precursor for terpene moiety formation, and GGPP could be used for biosynthesis of diterpenes, chlorophylls, phylloquinone, and plastoquinone (Lange and Ghassemian, 2003) or in protein prenylation like geranylgeranylation (Gerber et al., 2009). As GGPPSs are known to have an ability to use other allylic diphosphates such as GPP and FPP in addition to DMAPP (Ogura and Koyama, 1998; Takaya et al., 2003; Schmidt et al., 2010), enzyme assays and product verification showed that CrGPPS.LSU produced GGPP by utilizing both GPP and FPP in the presence of IPP, suggesting that reaction proceeds by sequential incorporation of IPP units (Figure 4G). The GGPPS activity of CrGPPS.LSU was further confirmed by *in vivo* genetic complementation (Figure 5). The transformants carrying pACCAR25ΔcrtE and human GGPPS (HsGGPPS, positive control) are expected to accumulate yellow pigmentation, confirming the substitution of *crtE*, whereas cells harboring pACCAR25ΔcrtE and CrGPPS.SSU/pET28a empty vector were used as negative controls. Cotransformation of CrGPPS.LSU (which is the same as CrGGPPS reported by Thabet et al., 2012) with pACCAR25ΔcrtE resulted in accumulation of yellow pigmentation (Figure 5B), confirming the *in vitro* assay data that CrGPPS.LSU has a GGPPS activity. Although, *M. piperita* heteromeric GPPS produced both GPP and GGPP in *in vitro* assays, the genetic complementation in *E. coli* did not show any detectable GGPPS activity (Chang et al., 2010).

In contrast to CrGPPS.LSU forming GPP and GGPP, the LSU of *A. majus* GPPS produced only GGPP (Tholl et al., 2004; Orlova et al., 2009) whereas LSU from *H. lupulus* GPPS formed GPP, FPP, and GGPP (Wang and Dixon, 2009). It is known that most short-chain prenyltransferases produce only a single main product (GPP or FPP or GGPP) but some homomeric prenyltransferases found in *Zea mays* and *P. abies*, and heteromeric GPPS from *H. lupus* and *M. Piperita*, make products with one more or one fewer C_5 units than the main product (Cervantes-Cervantes et al., 2006; Schmidt and Gershenzon, 2008; Wang and Dixon, 2009; Chang et al., 2010). Unlike other bifunctional enzymes stated above, CrGPPS.LSU is functionally similar to a recently reported phylogenetically distant gymnosperm PaIDS1 from *P. abies*, which showed bifunctional activity forming products GPP and GGPP (9:1 ratio) that differ from each other in size by more than C_5 unit (Schmidt et al., 2010). In this context, PaIDS1 and CrGPPS.LSU belong to an unusual class of short-chain prenyltransferases that make two major products with a difference of more than C_5 unit (Schmidt et al., 2010). This is the first report demonstrating the 'catalytic promiscuity' of an angiosperm prenyltransferase where the enzyme has the ability to catalyze an adventitious secondary activity (GPPS) at the active site responsible for the primary activity (GGPPS) (Copley, 2003; Schmidt et al., 2010). This 'catalytic promiscuity' of CrGPPS.LSU suggests its possible involvement in primary as well as secondary metabolism during the course of growth and development of *C. roseus.* The overexpression of snapdragon GPPS.SSU changed the chain length specificity of endogenous GGPPSs into GPPS leading to enhanced

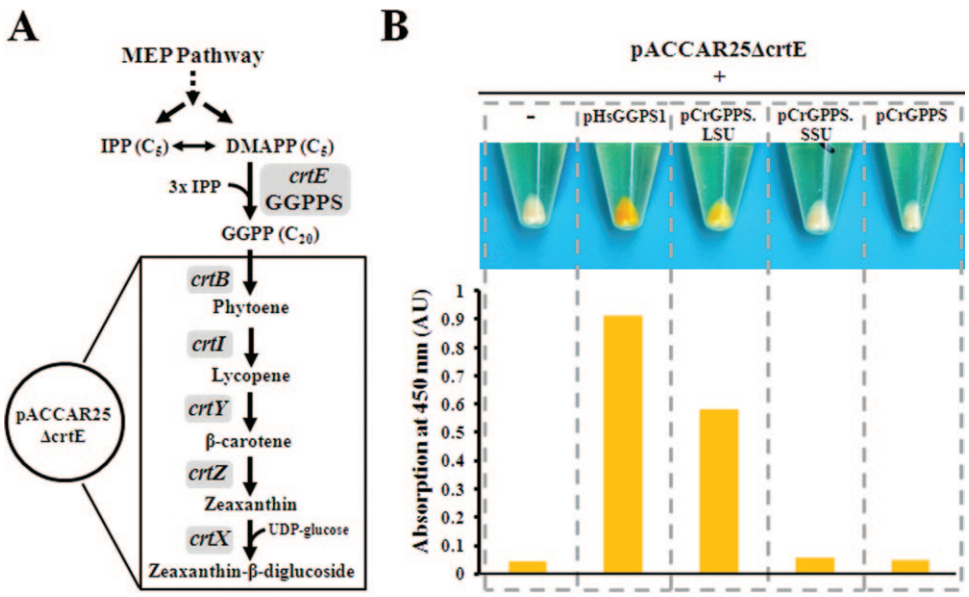

Figure 5. *In Vivo* Genetic Complementation Assay for Detecting GGPPS Activity.
(A) Schematic diagram for the carotenoid biosynthesis pathway, beginning with a coupled reaction of two C_{20}–GGPP molecules and the construct pACCAR25ΔcrtE.
(B) Genetic complementation assay for detecting yellow pigment production in *E. coli* harboring pACCAR25ΔcrtE and CrGPPSs expression vectors. Human GGPPS1 (pHsGGPPS1) and empty pET28a vector were used as positive and negative controls, respectively.

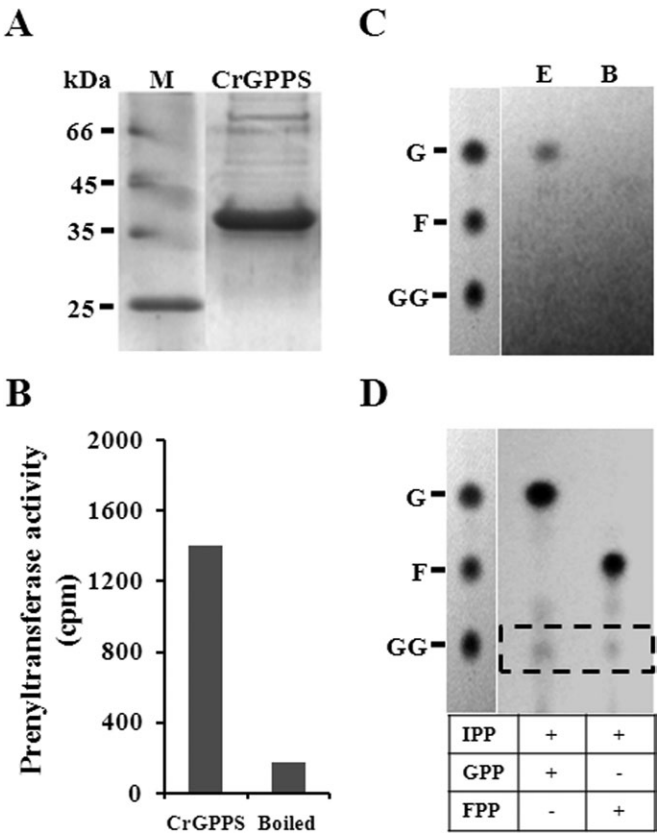

Figure 6. Purification, Enzyme Activity, and In Vitro Product Analysis of Homomeric CrGPPS.

(A) SDS–PAGE analysis of purified recombinant CrGPPS from *E. coli.*

(B) Enzyme activity of purified recombinant CrGPPS assayed with [1-$_3$H]-IPP and DMAPP.

(C) TLC analysis of reaction products from *in vitro* assays of purified CrGPPS in the presence of IPP and DMAPP.

(D) TLC analysis of products from *in vitro* assays of purified CrGPPS in the presence (+) or absence (–) of GPP/FPP with IPP. The product formed is indicated by a dashed box, while other spots are unreacted substrates. Products were hydrolyzed enzymatically, and the resulting alcohols were analyzed by TLC. The products were confirmed by comparing the spots with authentic standards G (geranol), F (farnesol), and GG (geranylgeranol). The boiled protein is used as negative control. E, enzyme; B, boiled enzyme.

monoterpene formation, but at the expense of primary metabolism (Orlova et al., 2009). It was suggested that the *in vivo* formation of heteromeric GPPS complex between the introduced snapdragon GPPS.SSU and tobacco GGPPSs redirected the metabolic flux to GPP formation consequently depleting the GGPP pool needed for primary metabolism (Orlova et al., 2009). Thus, efforts through metabolic engineering of dual G(G)PP synthase could increase both GPP and GGPP pool without affecting the primary metabolism in *C. roseus*.

To characterize the product formation by the heteromeric CrGPPS.SSU/CrGPPS.LSU complex, the co-purified proteins were used for prenyltransferase assays, which showed GPP as the exclusive product (Figure 4C). This is consistent with earlier reports on heteromeric GPPS from *A. majus* (Tholl et al., 2004) and in contrast to observations with heteromeric GPPS from *H. lupulus* and *M. piperita* that produced both GPP and GGPP and trace amounts of FPP (Wang and Dixon, 2009; Chang et al., 2010). These results indicated that catalytically active GPPS in *C. roseus* is present as a heteromer, which consists of inactive CrGPPS.SSU as a small subunit and an active bifunctional G(G)PPS as a large subunit. The interaction between CrGPPS.LSU and CrGPPS.SSU modified the chain length specificity of CrGPPS.LSU resulting in the exclusive production of GPP from IPP and DMAPP (Figure 4C). It has been shown in the structure of heteromeric GPPS from *M. piperita* that SSU restricts the connection between active site cavity and elongation cavity thereby limiting the catalytic reaction to go beyond C_{10}-GPP (Chang et al., 2010). Similarly, in *C. roseus*, it is possible that the interaction of CrGPPS.SSU alters the catalytic site of CrGPPS.LSU in their subunit architecture and confined the enzyme specificity to the formation of only GPP (Figure 4C). Moreover, the complex formation suggests that CrGPPS.SSU has a strong affinity to CrGPPS.LSU and could control CrGPPS.LSU homomerization. Our results show that CrGPPS.LSU per se is a functional GGPPS, which may be involved in primary metabolism, but to some extent could also contribute to secondary metabolism with its ability to release a substantial portion of the intermediate GPP, similarly to PaIDS1 (Schmidt et al., 2010). However, formation of a heteromer with CrGPPS.SSU resulting in highly efficient GPPS could contribute to the major redirection of flux to secondary metabolism.

Heterologous Expression and Functional Characterization of Homomeric CrGPPS

For functional characterization of homomeric CrGPPS, the open reading frame was cloned into expression vector pET28a having an N-terminal $(His)_6$-tag. The cloned construct was transformed into *E. coli* and the recombinant CrGPPS was expressed as a $(His)_6$-tag fusion protein. The full-length recombinant CrGPPS protein was completely insoluble (data not shown). A truncated version of CrGPPS starting from second methionine (Met_{100}–CrGPPS), and containing a $(His)_6$-tag, was expressed in *E. coli*. The truncation was based on earlier reports of *A. grandis* GPPS and LeGPS where truncation did not affect the catalytic activity and product profile (Burke and Croteau, 2002a; van Schie et al., 2007). The assay with purified recombinant CrGPPS proteins using [1-^{3}H]-IPP and DMAPP as substrates showed prenyltransferase activity (Figure 6A and 6B). While the purified recombinant CrGPPS produced GPP as the sole product with IPP and DMAPP as substrates (Figure 6C), it produced trace amounts of GGPP in the presence of either GPP or FPP along with IPP (Figure 6D). Both CrGPPS.LSU and CrGPPS showed preference for Mg^{2+} over Mn^{2+} and K^+ as cofactor similarly to other prenyltransferases (Supplemental Figure 1). The formation of only GPP by CrGPPS with IPP and DMAPP as substrates is in contrast to other homomeric GPPSs of the same clade represented by LeGPS, QrIDS1, and PaIDS3, which produced substantial

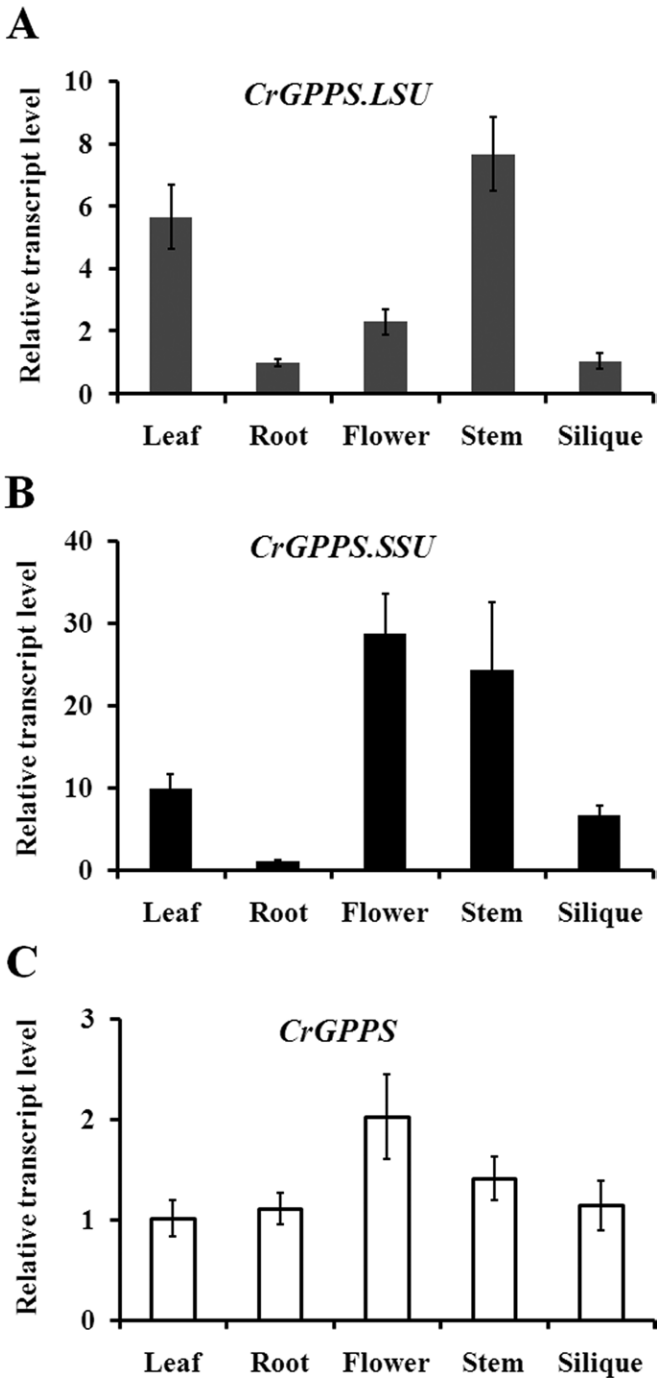

Figure 7. Tissue-Specific Expression of *CrGPPS.LSU, CrGPPS.SSU*, and *CrGPPS* Transcripts.

Quantitative RT–PCR analysis in different tissues of *C. roseus CrGPPS.LSU* **(A)**, *CrGPPS.SSU* **(B)**, and *CrGPPS* **(C)**. Relative transcript levels of *CrGPPS* genes in leaf, root, flower, stem, and silique were determined using the comparative Ct method. The error bar shows the standard errors from two biological replicates.

amounts of GPP, FPP, and GGPP (van Schie et al., 2007; Schmidt and Gershenzon, 2008), whereas an *Arabidopsis* prenyltransferase that was thought to be a GPPS earlier (Bouvier et al., 2000) but shown to be a polyprenyl pyrophosphate synthase (PPPS) recently produced no product (Hsieh et al., 2011). Also, a homomeric PbGDPS lacking substrate binding motifs (FARM and SARM) catalyzed GPP and trace FPP formation with IPP and DMAPP (Hsiao et al., 2008). However, a homomeric GPPS, PaIDS2 belonging to a different clade has the same product profile as that of CrGPPS with GPP as the sole product (Schmidt and Gershenzon, 2008). The production of a trace amount of GGPP by CrGPPS when incubated with GPP/FPP and IPP prompted us to check whether CrGPPS has any *in vivo* GGPPS activity. The genetic complementation assay showed no detectable yellow pigmentation in transformants carrying CrGPPS and pACCAR25ΔcrtE constructs similarly to negative controls (Figure 5B), suggesting that CrGPPS is a bona fide GPPS. Interestingly, none of the homomeric GPPSs present in the same clade along with CrGPPS is involved in monoterpene biosynthesis and it is evident from earlier studies that GPPSs from tomato (van Schie et al., 2007), *P. abies* (PaIDS3), and *Q. robur* (QrIDS1) were shown to be involved in diterpene formation (Schmidt and Gershenzon, 2008).

Spatio-Temporal Expression of CrGPPS Encoding Genes

The biosynthesis of MIAs in *C. roseus* is regulated tissue-specifically and developmentally (De Luca and St-Pierre, 2000; Facchini, 2001; Roepke et al., 2010). The complex MIA biosynthetic pathway is compartmentalized in multiple cell types of different organs such as shoots, leaves, and flowers (St-Pierre et al., 1999). To determine the contribution of *CrGPPS* genes in MIA formation, the mRNA expression was analyzed in different tissues and developmental stages, and in leaves treated with MeJA (a known alkaloid pathway regulator) by quantitative real-time PCR using gene-specific primers. With respect to tissue specificity, *CrGPPS.LSU* showed highest expression in stem and leaf followed by flower, with least expression in siliques and roots (Figure 7A). *CrGPPS.SSU* exhibited highest expression in flowers followed by stem, leaf, and silique, with least expression in roots (Figure 7B). *CrGPPS* was constitutively expressed in all tissues tested (Figure 7C). In earlier studies, the gene encoding SSUs of all characterized heteromeric GPPSs and a homomeric GPPS from orchid have shown tissue-specific expression in flowers (Tholl et al., 2004; Hsiao et al., 2008) or in trichomes (Wang and Dixon, 2009) that are the sites of monoterpene biosynthesis and emission. However, *CrGPPS.SSU* showed broad tissue specificity, with highest expression in flowers, followed by stem and leaf, indicating its possible involvement in floral monoterpene emission as well as in MIA formation. Young developing leaves are the sites of MIA biosynthesis and regulation of the MIA pathway at cell-, development-, and organ-specific levels, which suggests that the pathway gene expression is coupled to the secretory mechanisms of vindoline and catharanthine (De Luca and St-Pierre, 2000; Roepke et al., 2010). The accumulation of vindoline and catharanthine has been shown to increase with leaf age during early leaf

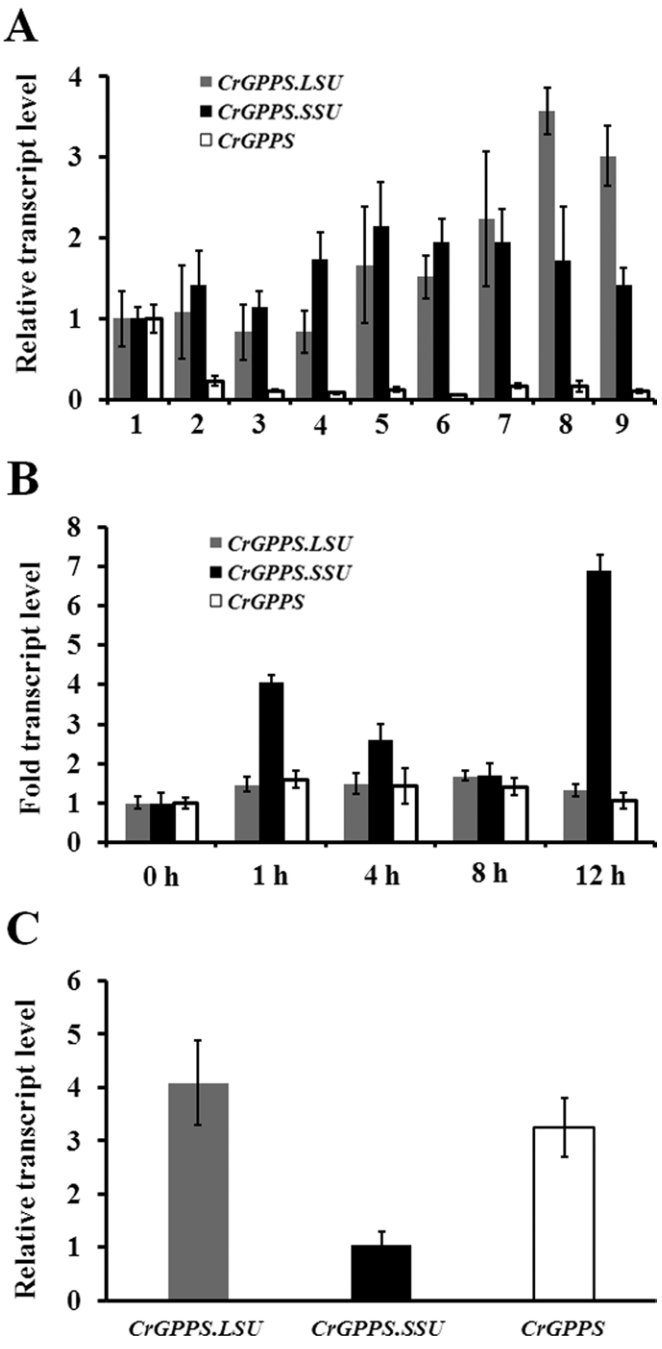

Figure 8. Relative Expression of *CrGPPS.LSU, CrGPPS.SSU*, and *CrGPPS* during Leaf Development and in Response to MeJA Treatment.

(A) Expression analysis of transcript levels of *CrGPPS.LSU, CrGPPS.SSU*, and *CrGPPS* in leaves of different developmental stages (leaf pairs 1, 2, 3, 4, 5, 6, 7, 8, and 9). The values were normalized to expression in the first leaf stage (= 1).

(B) qRT–PCR analysis of *CrGPPS.LSU, CrGPPS.SSU*, and *CrGPPS* gene expression in *C. roseus* leaves treated with MeJA. Expression profile is displayed as a relative expression compared to untreated leaves. The measured time points were 0, 1, 4, 8, and 12 h.

(C) Quantitative RT–PCR analyses to show relative expression of *CrGPPS. LSU, CrGPPS.SSU*, and *CrGPPS* in C. roseus leaves. The values were normalized to expression of *SSU* (= 1) that showed the least expression.

development (up to third-leaf age) and gradually declined reaching to ~40% of the maximum in older leaves (Roepke et al., 2010). When expression levels of mRNAs for *CrGPPS* genes were analyzed in leaves of different developing stages (from the first pair to the ninth pair of developing leaves), *CrGPPS.SSU* showed an increasing trend, reaching a maximum in the fifth-leaf pair, and declined slightly thereafter (Figure 8A), which more or less corresponded with the accumulation profile of vindoline and catharanthine (Roepke et al., 2010). In contrast, the expression of *CrGPPS. LSU* and *CrGPPS* showed reverse trends, with *CrGPPS.LSU* showing increased expression in older leaves and CrGPPS3 with higher expression in younger leaves (Figure 8A).

MeJA is a known inducer of MIA pathway resulting in the induced production of MIAs in *C. roseus* seedlings (Aerts et al., 1994), in hairy root cultures (Rijhwani and Shanks, 1998), in detached leaves (El-Sayed and Verpoorte, 2005), and in cell cultures (Rischer et al., 2006). Moreover, MeJA stimulates expression of enzymes associated with transcription factor-controlled accumulation of terpenoids and also is known to modulate expression of genes of early steps of terpene biosynthesis (reviewed in Hemmerlin et al., 2012). To determine the role of *CrGPPS* genes in the induced formation of MIAs, transcript levels were measured over a 12-h time course after leaves were treated with MeJA. Relative expression levels of *CrGPPS* genes were compared with those of control (Figure 8B). Unlike *CrGPPS.LSU* and *CrGPPS* that remained relatively constant after MeJA treatment, *CrGPPS.SSU* expression showed a rapid induction in a biphasic kinetic manner, with an immediate induction after 1 h followed by a decrease at 4 h and 8 h and dramatically peaking at 12 h (Figure 8B). A similar biphasic induction pattern was previously observed for octadecanoid-responsive *Catharanthus* AP-2 domain *ORCA2* (Menke et al., 1999), *ORCA3* (van der Fits and Memelink, 2001), and *TDC* and *STR* transcripts (Dutta et al., 2007). Also, ESMB (Early Steps in Monoterpene Biosynthesis) genes such as 1-deoxy-D-xylulose 5-phosphate synthase (*DXS2*) (Chahed et al., 2000), 1-deoxy-D-xylulose 5-phosphate reductase (*DXR*) (Veau et al., 2000), 2C-methyl-D-erythrol-2,4-cyclodiphosphate synthase (*MECS*), and 1-hydroxy-2-methyl-2-(E)-butenyl 4-diphosphate synthase (*HDS*), and geraniol 10-hydroxylase (*G10H*) have shown induced expression in response to MeJA (Rischer et al., 2006; Oudin et al., 2007). Moreover, a genome-wide transcript profiling by cDNA-amplified fragment-length polymorphisms (AFLP) with metabolic profiling of MeJA elicited *C. roseus* cell cultures showed an induced transcript accumulation of *ORCA2* and *ORCA3* and of genes encoding ESMB enzymes such as MECS, HDS, GPPS, G10H, and 10-hydroxygeraniol oxidoreductase (10HGO) (Rischer et al., 2006), in which the AFLP fragment annotated as *GPPS* in their study corresponded to *CrGPPS.SSU.* Endogenous GPPS enzyme activity was increased after MeJA application in *P. Abies*, suggesting that GPP produced by this enzyme is an important substrate for monoterpene biosynthesis in oleoresin production (Martin et al., 2002). The results

of spatio-temporal gene expression analysis combined with MeJA induction experiments suggested that only *CrGPPS.SSU* could be involved in regulating GPP availability for MIA biosynthesis. This conclusion is in agreement with previous studies that expression of *SSU* but not *LSU* regulates monoterpene biosynthesis (Tholl et al., 2004; Orlova et al., 2009; Wang and Dixon, 2009). Since it is known that catharanthine and vindoline production occurs in young developing leaves (Roepke et al., 2010), their relative transcript abundance in leaves of the third developmental stage was measured, which showed that, of the three genes, *CrGPPS.LSU* exhibited the highest expression, followed by *CrGPPS* and with lowest expression for *CrGPPS.SSU* (Figure 8C). Relative to *CrGPPS.LSU*, the low level of *CrGPPS.SSU* expression in contrast to other reported highly expressing *SSU*s of snapdragon, mint, and hop suggests that, in *C. roseus*, GPP formation is regulated in a different manner.

Effect of Transient Overexpression of *AmGPPS.SSU* in *C. roseus* Leaves

The SSU of heteromeric GPPS is known to interact with phylogenetically distant GGPPS proteins and modify the chain length specificity resulting in enhanced GPPS activity (Burke and Croteau, 2002b; Tholl et al., 2004; Wang and Dixon, 2009; Orlova et al., 2009). To determine whether AmGPPS.SSU interacts with CrGPPS.LSU, constructs carrying CrGPPS.LSU with a $(His)_6$-tag and AmGPPS.SSU without $(His)_6$-tag were co-expressed in *E. coli* and purified by Ni-NTA chromatography. The SDS–PAGE analysis (Figure 9A) and activity assays showed that CrGPPS.LSU interacted with AmGPPS.SSU, resulting in an active heteromeric GPPS that produced exclusively GPP from IPP and DMAPP (Figure 9B). In heteromeric GPPSs, SSU acts as a regulatory unit in controlling the flux to GPP for monoterpene production in specialized tissues such as trichomes of *Mentha* and hop, and petals of snapdragon flowers (Tholl et al., 2004; Orlova et al., 2009; Wang and Dixon, 2009). Since AmGPPS.SSU interacted with CrGPPS.LSU *in vitro* resulting in heteromeric GPPS, we transiently overexpressed AmGPPS.SSU in *C. roseus* leaves by Agroinfiltration. Transient overexpression of TDC and STR1 has been successfully demonstrated earlier in *C. roseus* leaves by Agroinfiltration (Di Fiore et al., 2004). Analysis of mRNA expression in *C. roseus* leaves infiltrated with *Agrobacterium tumefaciens* carrying the *AmGPPS.SSU* gene under the control of *C. breweri* LIS promoter (Orlova et al., 2006) showed high levels of *AmGPPS.SSU* transcripts after 2 d of infiltration (Figure 9C). Subsequent quantification of vindoline by High Performance Liquid Chromatography (HPLC) analysis in *AmGPPS.SSU* overexpressing leaves showed an improved vindoline (45%) content relative to controls (tissue infiltrated with *Agrobacteria* alone) (Figure 9D). This suggested that the introduced AmGPPS.SSU interacted with the endogenous CrGPPS.LSU, resulting in increased endogenous GPPS activity leading to improved availability of GPP for MIA biosynthesis. Thus, GPPS, being the

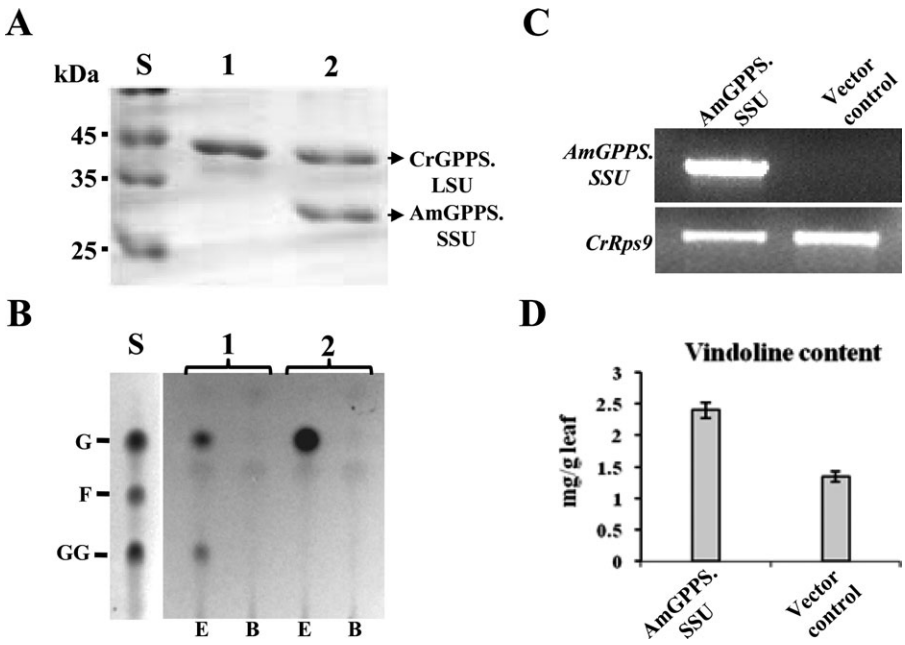

Figure 9. Transient Overexpression of AmGPPS.SSU in *C. roseus* Leaves.
(A) SDS–PAGE analysis showing co-purified band of heteromeric complex containing CrGPPS.LSU and AmGPPS.SSU.
(B) TLC analysis of reaction products from *in vitro* assays using the CrGPPS.LSU (panel 1) and CrGPPS.LSU/AmGPPS.SSU complex (panel 2) in presence of IPP and DMAPP. Semi-quantitative RT–PCR analysis **(C)** and vindoline content **(D)** in *C. roseus* leaves infiltrated with *Agrobacterium* carrying a *AmGPPSS.SSU* overexpression construct and control leaves infiltrated with *Agrobacterium* carrying empty vector. Analysis was carried out 48 h post infiltration.

branch-point enzyme for monoterpene moiety formation, could control the flux towards MIA formation.

Subcellular Localization of *C. roseus* GPPS Proteins

The biochemical characterization of CrGPPS proteins showed that they may participate in the formation of GPP *in vivo*—a process that is generally accepted to take place in plastids by utilizing IPP and DMAPP derived from the MEP pathway (Eisenreich et al., 1997). *In silico* analysis of CrGPPS amino acid sequences using various prediction programs revealed that CrGPPS.LSU and CrGPPS.SSU were predicted to be localized in the chloroplast, whereas CrGPPS had a high possibility of mitochondrial localization (Supplemental Table 1). Moreover, analysis of sequences of characterized homomeric GPPSs from *A. thaliana*, *L. esculentum*, *Q. robur*, *P. abies* (PaIDS2), and *A. grandis* also predicted their localization in mitochondria (Supplemental Table 1). The localization of CrGPPS.LSU has been shown to be plastidial in a previous study (Thabet et al., 2012), where they have annotated it as CrGGPPS. To determine the subcellular localization of the other two proteins, the first 100- and 142-aa sequences of CrGPPS.SSU and CrGPPS, respectively, were fused to the N-terminus of 326-sGFP under the control of CaMV 35S promoter. Transient overexpression of corresponding fusion proteins in *A. thaliana* protoplasts exhibited the GFP fluorescence in chloroplasts for CrGPPS.SSU (Figure 10). The plastidial localization of both subunits of heteromeric CrGPPS is consistent with earlier reports from SSU of *A. majus* and SSU and LSU of GPPSs from *M. piperita* and *H. lupulus* (Tholl et al., 2004; Turner and Croteau, 2004; Wang and Dixon, 2009).

Unlike CrGPPS.LSU and CrGPPS.SSU, CrGPPS–GFP fusion protein exhibited a punctuate pattern of fluorescence indicating mitochondrial localization (Figure 10), which is consistent with all prediction programs (Supplemental Table 1). This is the first report of localization of a homomeric GPPS in plants. Although GGPPS enzymes are present mainly in plastids (Okada et al., 2000; Tholl et al., 2004; Ament et al., 2006; Pateraki and Kanellis, 2008; Orlova et al., 2009; Thabet et al., 2012), one of the isozymes from *A. thaliana* has shown to be localized in mitochondria (Okada et al., 2000). Similarly to *A. thaliana*, *C. roseus* seems to possess multiple GGPPS isozymes (Figure 11) and their exact localization and role in isoprenoid biosynthesis remain to be determined. Recently, two isoforms of IPP isomerase encoded by a single gene have been shown to possess unique triple localization in plastids, mitochondria, and peroxisomes in *C. roseus* (Guirimand et al., 2012). The results from this study, and from previous studies with FPPS, GGPPS, isopentenyl diphosphate isomerase (IDI), and GES localization (Thabet et al., 2011; Guirimand et al., 2012; Simkin et al., 2012; Thabet et al., 2012), suggested that the terpenoid pathway branches are spread across different subcellular compartments in *C. roseus* and their precursors might be synthesized in the associated organelles themselves. Hence, in plants, the presence of CrIDI, CrGPPS, and AtGGPPS6 in mitochondria implies the existence of an associated isoprenoid biosynthetic pathway which serves as a precursor for isoprenoid quinones involved in electron transfer system (Okada et al., 2000). It is possible that GPP produced by GPPS is preferentially used by mitochondrial GGPPS, as an allylic substrate, rather than DMAPP (Hemmerlin et al., 2012).

Phylogenetic Relationships of CrGPPSs

Genes encoding GPPS enzymes have been isolated and characterized in select members of plants belonging to both angiosperms and gymnosperms, which are mostly known to produce high amounts of monoterpenes. Based on their sequence comparison and prenyltransferase activity, it has

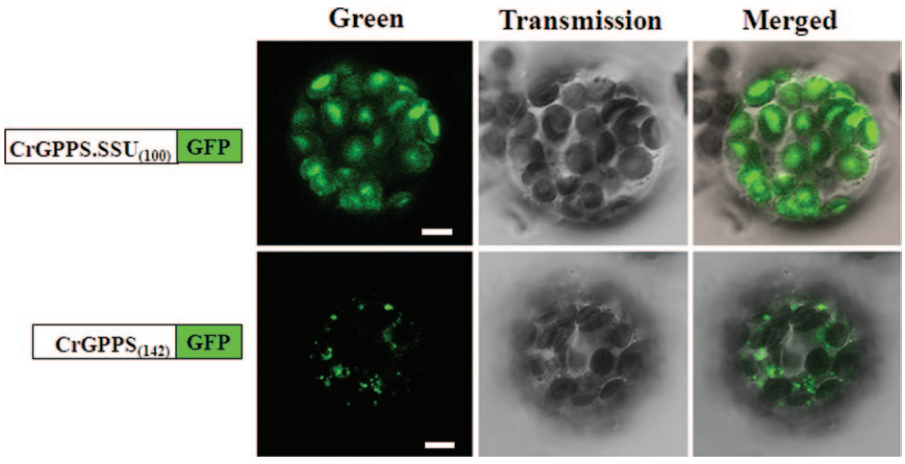

Figure 10. Confocal Laser Scanning Microscopy of Transiently Expressed CrGPPS.SSU–GFP and CrGPPS–GFP Fusions in Arabidopsis Protoplasts.
GFP fusion constructs are shown on the left, and the corresponding transient expression in the protoplast is shown on the right. Green fluorescent protein fluorescence detected in the green channel is shown in the 'Green' column; the 'Transmission' column shows light-microscopy images of intact protoplasts. Scale bars = 50 μm. The numbers in the fusion constructs correspond to amino acid positions.

been suggested that plant GPPSs might have multiple origins during the course of evolution (Tholl et al., 2004) with an ability to produce monoterpenes in specialized organs (Wang and Dixon, 2009). Although GPPS enzymes have been characterized in angiosperm and gymnosperms, the type/s of GPPS enzymes and its/their role in MIA producing plant is not yet reported. A phylogenetic analysis of CrGPPS proteins with all characterized GPPS sequences revealed three major clades of isoprenyl diphosphate synthases (IDS): IDS-a, IDS-b, and IDS-c (Figure 11). IDS-a is subdivided into IDS-a1 and IDS-a2 based on the enzyme activity and evolutionary relatedness. IDS-a1 clade consists of enzymes from angiosperms and is represented by LSUs of heteromeric GPPS and GGPPS (Burke et al., 1999; Tholl et al., 2004; Wang and Dixon, 2009; Orlova et al., 2009). All candidates of IDS-a1 produced GGPP as the major product with the exception of CrGPPS.LSU, which predominantly produced GPP (Figure 11). IDS-a2 representing homomeric GPPS is found only in conifers, which includes GPPSs from *A. grandis* (Burke and Croteau, 2002a) and *P. abies* (Schmidt and Gershenzon, 2008; Schmidt et al., 2010). Interestingly, all enzymes of IDS-a2 produced GPP as the predominant product in addition to FPP and GGPP with the exception of PaIDS1, which is reported to be a bifunctional G(G)PPS producing substantial amounts of GPP and GGPP. CrGPPS.LSU and PaIDS1, being in two different sub-clades, display the catalytic promiscuity having bifunctional enzymatic activity producing GPP and GGPP. CrGPPS falls

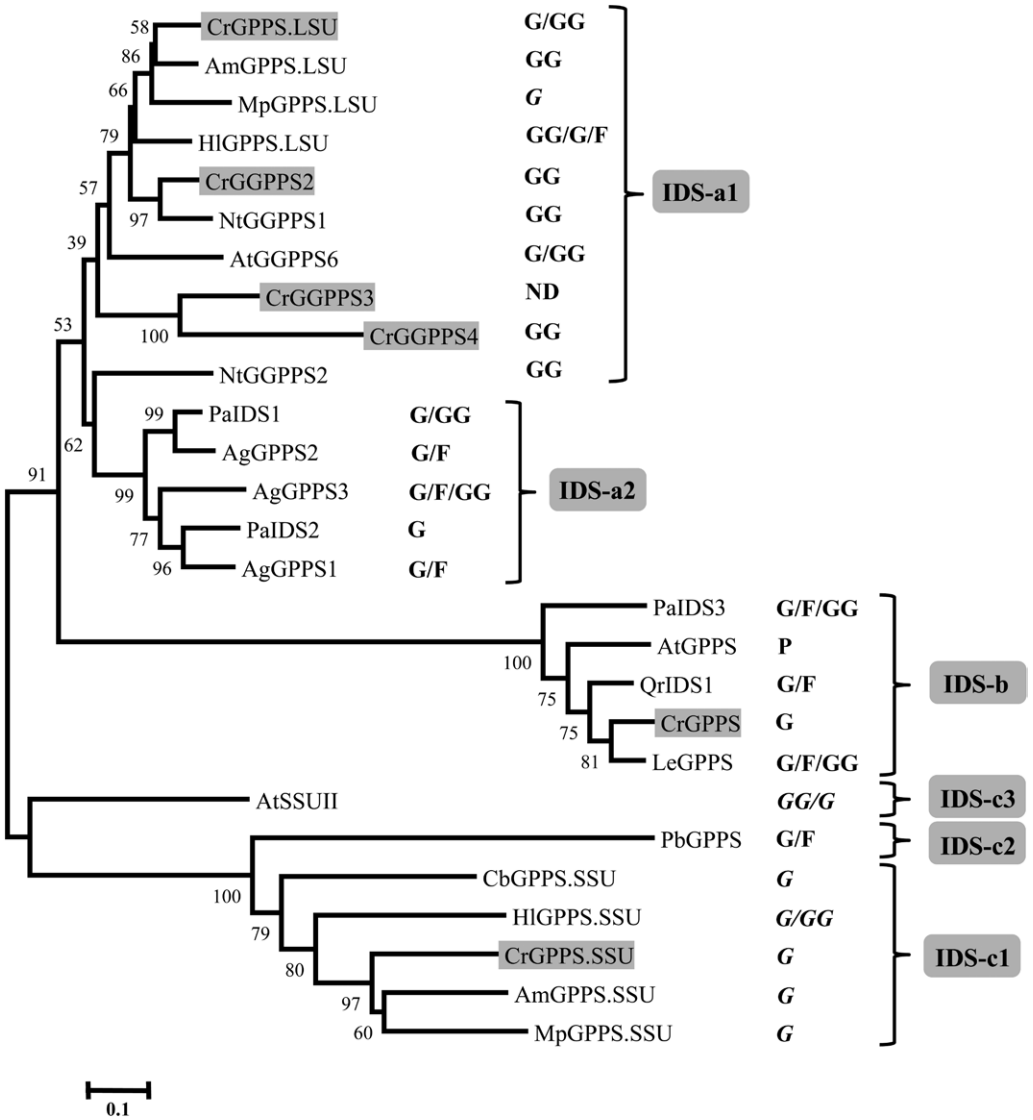

Figure 11. Phylogenetic Analysis of Amino Acid Sequences of Homomeric and Heteromeric Plant GPPSs.
A phylogenetic tree was constructed by the neighbor-joining method using default settings of MEGA 4.0 (Tamura et al., 2007). The branch length of the line indicates evolutionary distances, and numbers represent the confidence of the phylogenetic tree calculated by bootstrap analysis from 1000 replicates. The abbreviation and accession number used in constructing the phylogenetic tree are given in the 'Methods' section. Products generated by different short-chain prenyltransferases are represented by G/F/GG in order of their abundance. Products generated by heteromeric complexes involving SSUs are shown in italics. IDS, isoprenyl diphosphate synthase. G, F, and GG represent GPP, FPP, and GGPP, respectively.

into IDS-b clade that includes three angiosperm GPPSs from *Arabidopsis* (AtGPPS), *L. esculentum* (LeGPS), and *Q. rubur* (QrIDS1), and one gymnosperm GPPS from *P. abies* (PaIDS3), which produced FPP and or GGPP in addition to GPP (Bouvier et al., 2000; van Schie et al., 2007; Schmidt and Gershenzon, 2008). AtGPPS was recently shown to be a PPPS in contrast to the earlier report (Hsieh et al., 2011). However, CrGPPS from the same IDS-b clade produced only GPP and showed mitochondrial localization (Figure 10 and Figure 11). Interestingly, prediction analyses revealed that, like CrGPPS, the GPPSs of *A. grandis* (AgGPPS1) of clade-IDSa2 and all proteins of clade IDS-b seem to be localized to mitochondria (Supplemental Table 1). This suggested the possible role of IDS-a2 and IDS-b clade of enzymes in associated terpene biosynthesis pathways in plant cell. The IDS-c1 is represented by inactive SSU-I class of heteromoeric GPPS, whereas an unusual homomeric GPPS from orchid (*P. bellina*) lacking a $DD(X)_{2-4}D$ motif with close relatedness to SSUs has been clustered as IDS-c2 clade (Hsiao et al., 2008). The IDS-c3 clade contains a unique *A. thaliana* protein (AtSSU-II) with two CxxxC motifs and a FARM motif but lacking a SARM motif (Wang and Dixon, 2009) (Figure 11). AtSSU-II showed no activity but modified the chain length specificity of AtGGPPS11 and HlGPPS.LSU, which is similar to the function of other characterized SSUs (Wang and Dixon, 2009). Our phylogenetic analysis demonstrated that IDS-c clade, consisting of members of IDS-c1, IDS-c2, and IDS-c3, could have evolved from a common ancestor in which a homodimeric GPPS falling into IDS-c2 clade is active whereas SSU-I (IDS-c1) and SSU-II (IDS-c3) are catalytically inactive. This could be due to the exceptionally high speciation rate of orchids (Tsai and Chen, 2006) that would have altered the inactive SSU by modification of a few amino acids, resulting in the required GPPS activity. This is evident with the presence of an alternate EAEVE motif of PbGPPS, which is located in the equivalent position of SARM (Hsiao et al., 2008). The significance of presence of SSU-II in plants is currently unknown but a systematic characterization of this class in different plants should provide the evidence for its role in plant metabolism.

Conclusions

The study of complex MIA biosynthesis and its regulation remains a great challenge in plant secondary metabolism. The functional characterization of CrGPPSs in this study provided insights into the formation of GPP in *C. roseus*. The CrGPPS.LSU might have evolved to produce both GPP and GGPP in *C. roseus* to maintain relative amounts of precursors for both primary as well as secondary metabolism. The plastid targeted CrGPPS.SSU and CrGPPS.LSU form active heteromeric GPPS to catalyze efficient production of GPP *in vivo* and provide better availability of this substrate to geraniol synthase, whereas homomeric CrGPPS might be involved in mitochondrial isoprenoid biosynthesis for the production of ubiquinones. The temporal and spatial expression analysis of *CrGPPS* genes and transient overexpression implies that *CrGPPS.SSU* could function in coordinated redirection of the metabolic flux, thereby acting as a primary regulator to a certain extent in MIA biosynthesis. Taken together, our results suggest that, under normal conditions, a basal level of the GPP pool is provided by both CrGPPS.LSU (a bifunctional G(G)PPS) and heteromeric CrGPPS.LSU/CrGPPS.SSU towards MIA formation in *C. roseus*. However, under biotic/abiotic stress, the induced expression of SSU could result in an elevated level of GPPS activity by LSU and SSU interaction, thereby increasing the GPP pool towards MIA biosynthesis.

METHODS

Plant Material and MeJA Treatment

C. roseus cv. Dhawal (National Gene Bank, CSIR–CIMAP, India) plants were grown under normal greenhouse conditions. For MeJA treatments, 95% pure MeJA (Sigma-Aldrich) was added to a 5% (w/v) sucrose solution to a final concentration of 200 mM. Excised leaves of the third developmental stage were placed in a Petri plate containing the MeJA/sucrose or DMSO (the MeJA solvent) as a control. Samples were collected at 0, 1, 4, 8, and 12 h, and stored at –80°C until further use.

Chemicals and Radiochemicals

[1-^{3}H]-IPP (1.85 MBq) was purchased from American Radiolabeled Chemicals (www.arcincusa.com). Unlabeled IPP, DMAPP, GPP, and FPP were purchased from Echelon Research Laboratories (www.echelon-inc.com). Terpenoid standards and reagents were purchased from Sigma-Aldrich (www.sigmaaldrich.com) unless otherwise noted.

RNA Isolation and cDNA Synthesis

About 100 mg of tissue was ground in liquid nitrogen and total RNA was extracted using a Spectrum™ Plant Total RNA Kit (Sigma-Aldrich, USA) according to the manufacturer's instructions. To amplify the 3′ end of CrGPPS.SSU, 3′ RACE cDNA was prepared with 5 µg total RNA using a Superscript III RT Module (Invitrogen). Then, 3′ RACE PCR was carried out using a GeneRacer™ Kit (Invitrogen) with 3′ RACE cDNA along with gene-specific reverse and nested primers and GeneRacer 3′ and 3′ nested primers (Supplemental Table 2). The amplified fragment was cloned into pJET1.2/ vector and the sequence was confirmed by nucleotide sequencing. cDNA for amplifying open reading frames of CrGPPSs and for real-time PCR analysis was prepared by using a RevertAid™ H Minus First Strand cDNA Synthesis Kit (Fermentas International Inc., Canada). For real-time qRT–PCR, the DNA-free total RNA (5 µg) was used for first-strand cDNA synthesis with $Oligo(dT)_{18}$ primers using RevertAid H Minus Reverse Transcriptase. A linear range of cDNA was used for real-time PCR. Real-time qRT–PCR was performed in a 96-well plate using the Applied Biosystems 7900HT Fast Real-Time PCR System (PE Applied Biosystems, www.appliedbiosystems.com) with SYBR green fluorescent dye using respective forward and reverse primers for each gene (Supplemental Table 2). Fold change differences in gene

expression were analyzed using the comparative cycle threshold (Ct) method (Applied Biosystems). Each data point represents the mean of two independent biological replicates and three technical replicates. Real-time qRT–PCR conditions were as follows: 94°C for 10 min for one cycle, followed by 40 cycles of 94°C for 15 s, 54°C for 15 s, and 72°C for 15 s.

Phylogenetic Analysis

The deduced amino acid sequence were aligned using MEGA 4.0 (Tamura et al., 2007) with default settings. A phylogenetic tree was constructed with the neighbor-joining method using default settings of MEGA (Tamura et al., 2007). Bootstrap values were calculated from 1000 replicates. Shading of amino acid sequence alignment was done by BOXSHADE 3.21 version (www.ch.embnet.org/software/BOX_form.html).

Cloning of *GPPS* Genes and Generation of Overexpression Constructs

The open reading frame of each CrGPPS was amplified with a forward and a reverse primer consisting of the primers that included a start and stop codon along with restriction sites for cloning into pET28a vector. The primer combinations used are mentioned in Supplemental Table 2. PCR was performed using Platinum *Taq* DNA polymerase High Fidelity (Invitrogen) and PCR products were gel-purified using a gel extraction kit (Fermentas). PCR products were cloned into pJET 1.2/blunt cloning vector (CloneJET PCR cloning kit, Fermentas) and transformed into *E. coli* XL1 for plasmid amplification. After restriction digestion and gel extraction, resulting fragments were sub-cloned into the expression vector pET28a (Novagen) downstream and in-frame of $(His)_6$-tag or pET32a for non-$(His)_6$-tag clones. Positive clones were selected and the resulting constructs were confirmed by restriction digestion and nucleotide sequencing.

Expression and Purification of Recombinant Proteins

For functional expression, *E. coli* Rosetta-2 competent cells were transformed with recombinant plasmids and pET28a/pET32a lacking an insert (control). Induction, harvesting, and protein purification by affinity chromatography on nickel-nitrilotriacetic acid agarose (Bio-Rad, www.bio-rad.com) were performed as described by Nagegowda et al. (2008). Briefly, a single colony was used to inoculate 25 ml Luria-Bertani medium with 37 mg ml^{-1} chloramphenicol and 50 mg ml^{-1} ampicillin (for pET32a constructs) or 50 mg ml^{-1} kanamycin (for pET28a constructs) or with both antibiotics (for co-expression of both pET32a/pET28a constructs), which were grown overnight at 37°C. Five ml of these cultures were transferred to 1000 ml of the same medium and continued to grow at 37°C until an absorbance of 0.5 at $OD_{600\,nm}$. Cultures were then induced by the addition of isopropyl-1-thio-β-D-galactopyranoside (IPTG) to a final concentration of 0.4 mM and grown for an additional 18 h at 18°C. Protein purification by affinity chromatography on nickel-nitrilotriacetic (Ni-NTA) acid agarose (Bio-Rad) was performed. Protein concentration was determined using the Bradford method (Bradford, 1976).

Prenyltransferase Assays and Product Identification

Prenyltransferase assays were performed as described previously (Orlova et al., 2009) except for the use of 40 μM [1-^{3}H]-IPP instead of ^{14}C-IPP. The reaction was performed in a final volume of 100 μl containing 40 μM[1-^{3}H]-IPP (50 mCi $mmol^{-1}$) and 40 μM DMAPP in assay buffer (25 mM MOPSO, pH 7.0, 10% [v/v] glycerol, 2 mM DTT, and 10 mM $MgCl_2$). For the identification of reaction products, larger-scale assays were performed in a final volume of 200 μl containing 80 μM-IPP and 80 μM DMAPP in assay buffer (25 mM MOPSO, pH 7.0, 10% [v/v] glycerol, 2 mM DTT, and 10 mM $MgCl_2$). Assays were performed for 6 h at 30°C. To stop the assay and hydrolyze all diphosphate esters (including un-reacted substrate as well as products), 200 μl of a solution containing 2 units of bovine intestine alkaline phosphatase (18 units mg^{-1}; Sigma-Aldrich) and 2 units of potato apyrase (25.2 units mg^{-1}; Sigma-Aldrich) in 0.2 M Tris-HCl, pH 9.5, were added to samples followed by overnight incubation at 30°C. After enzymatic hydrolysis, the resulting prenyl alcohols were extracted with 1 ml hexane and the hexane fraction was concentrated to 25 μl. The products were separated on reversed-phase TLC plates (TLC Silica gel 60 RP-18 $F_{254}S$; MERCK, Germany). Chromatography was performed using a methanol:water (95:5 v/v) mobile phase, and spots were visualized by exposure of TLC plates to iodine vapor. Triplicate assays were performed for all data points. Enzyme assays were performed with one of following cations present in the assay buffer at final concentrations of 10 mM: Mg^{2+}, Mn^{2+}, or K^+. All results represent an average of three independent assays.

In Vivo Genetic Complementation Assay

The pACCAR25ΔcrtE (Kainou et al., 1999) which contain the gene cluster *crtX*, *crtY*, *crtI*, *crtB*, and *crtZ* encoding carotenoid biosynthetic enzymes except *crtE* encoding GGPPS were used for determining *in vivo* GGPPS activity. The pET28a–CrGPPS constructs or HsGGPPS/pBH (as positive controls) and pACCAR25ΔcrtE were co-transformed into *E. coli* BL21 (DE3) with respective antibiotics (chloramphenicol for pACCAR25ΔcrtE; ampicillin for HsGGPPS and pBH; kanamycin for pET28a construct of CrGPPS.LSU, CrGPPS.SSU, and CrGPPS) and plated on LB plates to grow overnight at 37°C. A single colony from plates containing transformed colonies was picked and used for growth and induction as mentioned in the earlier section. To quantify carotenoids, pellets were obtained after centrifugation and dissolved in 90% (v/v) acetone to extract pigments. The concentration of carotenoid was determined by absorption at 450 nm using a Bio-Rad SmartSpec Spectrophotometer (Chang et al., 2010).

Transient Overexpression of AmGPPS.SSU in *C. roseus* Leaves by Agroinfiltration

The plasmid pEF1.LIS–AmGPPS.SSU (Orlova et al., 2009) containing the coding region of snapdragon (*A. majus*) GPPS. SSU under *C. breweri* LIS promoter (1038 bp) (Orlova et al.,

2006) was used for transient expression in *C. roseus* leaves following the protocol of Long et al. (2009). Leaves from the third developmental stage of *C. roseus* were vacuum-infiltrated with *A. tumefaciens* strain GV3101 containing pEF1. LIS–AmGPPS.SSU and pEF1–LIS vector (control) for 15 min and kept for 36 h in the dark in 5% sucrose. The DNA-free total RNA from infiltrated leaves was isolated as described in the 'Methods' section. The expression of introduced *AmGPPS.SSU* was analyzed by semi-quantitative RT–PCR. Extraction of alkaloids from infiltrated leaves and determination of vindoline content by HPLC were carried out using the protocol reported earlier (Singh et al., 2000; Gupta et al., 2005). Briefly, shade-dried leaves (1 g) were powdered and extracted thrice with 90% ethanol (3 × 30 ml, 12 h each time). The alcohol extract was filtered, concentrated to 10 ml, then acidified with 10 ml of 3% HCl and washed thrice with 30 ml hexane. The aqueous portion was basified with ammonia to pH 8.5 and extracted thrice using 30 ml chloroform. The chloroform extract was washed with water, dried over sodium sulfate, and concentrated under vacuum. The residue was re-dissolved in methanol. Methanolic extract and pre-filtered solvents were subjected to HPLC analysis using a Shimadzu LC-8A gradient HPLC equipped with LC-8A pumps, manual injector valve, SPD-M10*Avp* PDA detector, and RP-18e reversed-phase chromolith performance HPLC column.

Bioinformatic Analysis

The predictions of protein subcellular localization were performed using PSORT (http://psort.ims.u-tokyo.ac.jp/), Predotar (http://urgi.versailles.inra.fr/predotar/predotar.html), ChloroP 1.1 (www.cbs.dtu.dk/services/ChloroP/), MitoProt (http://ihg.gsf.de/ihg/mitoprot.html), and TargetP 1.1 (www.cbs.dtu.dk/services/TargetP/).

Subcellular Localization Studies

The subcellular localization of CrGPPSs was studied by generating green fluorescent fusion proteins in-frame with *Xba*I/*BamH*I cloning sites of the p326–SGFP vector containing the CaMV 35S promoter. Full-length ORF of CrGPPSs and their truncated variants were amplified with Platinum *Taq* DNA polymerase High Fidelity (Invitrogen) using respective primers described in Supplemental Table 2. Amplified fragments were cloned in-frame with the 5′ end of the GFP coding sequence to generate the CrGPPSs–GFP fusion protein and then sequenced to confirm accuracy of fusions. *Arabidopsis* protoplasts were prepared and transformed as described previously (Sheen, 2002; Nagegowda et al., 2008). DNA from each construct (10 μg) was used for PEG-mediated transformation of 100 μl of ice-cold protoplasts. p326–sGFP and p326–RbTP–SGFP were used as controls for cytosolic and plastidial localization. Transient expression of GFP fusion proteins was observed 16–20 h after transformation using a LSM 510 Meta confocal microscope with a 405 laser-Carl ZEISS in the Central Imaging and Flow Cytometry Facility at the National Centre for Biological Sciences (NCBS), Bangalore, India.

Accession Numbers

The GenBank accession numbers for the sequences mentioned in this article are as follows: AgGPPS1, AF51311; AgGPPS2, AF513112; AgGPPS3, AF513113; AmGPPS.SSU, AAS82859; AmGPPS.LSU, AAS82860; AtGGPPS6, At3g14530; AtGPPS, Y17376; AtSSU-II, At4g38460; CbGPPS.SSU, AY534745; CrGGPPS2, JX417186; CrGGPPS3, JX417187; CrGGPPS4, KC288140; CrGPPS, JX417185; CrGPPS.LSU, JX417183; CrGPPS.SSU, JX417184; HlSSU, ACQ90681; HlLSU, ACQ90682; LeGPS, DQ286930; MpGPPS.LSU, AF182828; MpGPPS.SSU, AF182827; NtGGPPS1, ADD49734; NtGGPPS2, ADD9735; PaIDS1, ACZ57571; PaIDS2, ACA21458; PaIDS3, ACA21459; PbGPPS, EU023907; and QrIDS1, CAC20852.

SUPPLEMENTARY DATA

Supplementary Data are available at *Molecular Plant Online.*

FUNDING

DAN thanks the Department of Biotechnology, Government of India, for the Ramalingaswami Fellowship (BT/HRD/35/24/2006). A.R. and A.K.S. are the recipients of a Research Fellowship from the University Grants Commission, and the Council of Scientific and Industrial Research, respectively.

ACKNOWLEDGMENTS

The authors are grateful to Dr C.S. Nautiyal, Director CSIR–CIMAP. D.A.N. expresses his sincere gratitude to Professor Ram Rajasekharan for his support and encouragement. Our special thanks go to Dr Ajit Shasany for sharing reagents. The authors are also thankful to Drs Natalia Dudareva, Inhwan Hwang, and Makoto Kawamukai for AmGPPS.SSU overexpression constructs, 326–sGFP, and pACCAR25ΔcrtE vectors, respectively. Confocal images were acquired at the Central Imaging and Flow Cytometry Facility, NCBS, Bangalore. We thank anonymous reviewers for their comments and suggestions. No conflict of interest declared.

REFERENCES

Aerts, R.J., Gisi, D., De Carolis, E., De Luca, V., and Baumann, T.W. (1994). Methyl jasmonate vapor increases the developmentally controlled synthesis of alkaloids in *Catharanthus* and *Cinchona* seedlings. Plant J. **5**, 635–643.

Ament, K., Van Schie, C.C., Bouwmeester, H.J., Haring, M.A., and Schuurink, R.C. (2006). Induction of a leaf specific geranylgeranyl pyrophosphate synthase and emission of (E,E)-4,8,12-trimethyltrideca-1,3,7,11-tetraene in tomato are dependent on both jasmonic acid and salicylic acid signaling pathways. Planta. **224**, 1197–1208.

Arvy, M.P., Imbault, N., Naudascher, F., Thiersault, M., and Doireau, P. (1994). 2,4-D and alkaloid accumulation in periwinkle cell suspensions. Biochimie. **76**, 410–416.

Bouvier, F., Suire, C., d'Harlingue, A., Backhaus, R.A., and Camara, B. (2000). Molecular cloning of geranyl diphosphate synthase and compartmentation of monoterpene synthesis in plant cells. Plant J. **24**, 241–252.

Bradford, M.M. (1976). A rapid and sensitive method for the quantitation of microgram quantities of protein utilizing the principle of protein–dye binding. Anal. Biochem. **72**, 248–254.

Burke, C.C., and Croteau, R. (2002a). Geranyl diphosphate synthase from *Abies grandis*: cDNA isolation, functional expression, and characterization. Arch. Biochem. Biophys. **405**, 130–136.

Burke, C.C., and Croteau, R. (2002b). Interaction with the small subunit of geranyl diphosphate synthase modifies the chain length specificity of geranylgeranyl diphosphate synthase to produce geranyl diphosphate. J. Biol. Chem. **277**, 3141–3149.

Burke, C.C., Wildung, M.R., and Croteau, R. (1999). Geranyl diphosphate synthase: cloning, expression, and characterization of this prenyltransferase as a heterodimer. Proc. Natl Acad. Sci. U S A. **96**, 13062–13067.

Cervantes-Cervantes, M., Gallagher, C.E., Zhu, C., and Wurtzel, E.T. (2006). Maize cDNAs expressed in endosperm encode functional farnesyl diphosphate synthase with geranylgeranyl diphosphate synthase activity. Plant Physiol. **141**, 220–231.

Chahed, L., Oudin, A., Guivarc'h, N., Hamdi, S., Chénieux, J., Rideau, M., and Clastre, M. (2000). Deoxy-D-xylulose 5-phosphate synthase from periwinkle: cDNA identification and induced gene expression in terpenoid indole alkaloid producing cells. Plant Physiol. Biochem. **38**, 559–566.

Chang, T.H., Hsieh, F.L., Ko, T.P., Teng, K.H., Liang, P.H., and Wang, A.H. (2010). Structure of a heterotetrameric geranyl pyrophosphate synthase from mint (*Mentha piperita*) reveals intersubunit regulation. Plant Cell. **22**, 454–467.

Copley, S.D. (2003). Enzymes with extra talents: moonlighting functions and catalytic promiscuity. Curr. Opin. Chem. Biol. **7**, 265–272.

De Luca, V., and St-Pierre, B. (2000). The cell and developmental biology of alkaloid biosynthesis. Trends Plant Sci. **5**, 168–173.

Di Fiore, S., Hoppmann, V., Fischer, R., and Schillberg, S. (2004). Transient gene expression of recombinant terpenoid indole alkaloid enzymes in *Catharanthus roseus* leaves. Plant Mol. Biol. Rep. **22**, 15–22.

Dudareva, N., Negre, F., Nagegowda, D.A., and Orlova, I. (2006). Plant volatiles: recent advances and future perspectives. Crit. Rev. Plant Sci. **25**, 417–440.

Dutta, A., Singh, D., Kumar, S., and Sen, J. (2007). Transcript profiling of terpenoid indole alkaloid pathway genes and regulators reveals strong expression of repressors in *Catharanthus roseus* cell cultures. Plant Cell Rep. **26**, 907–915.

Eisenreich, W., Sagner, S., Zenk, M.H., and Bacher, A. (1997). Monoterpenoid essential oils are not of mevalonoid origin. Tetrahedron Lett. **38**, 3889–3892.

El-Sayed, M., and Verpoorte, R. (2005). Methyljasmonate accelerates catabolism of monoterpenoid indole alkaloids in *Catharanthus roseus* during leaf processing. Fitoterapia. **76**, 83–90.

Facchini, P.J. (2001). Alkaloid biosynthesis in plants: biochemistry, cell biology, molecular regulation, and metabolic engineering applications. Annu. Rev. Plant. Physiol. Plant Mol. Biol. **52**, 29–66.

Facchini, P.J., and De Luca, V. (2008). Opium poppy and Madagascar periwinkle: model non-model systems to investigate alkaloid biosynthesis in plants. Plant J. **54**, 763–784.

Gerber, E., Hemmerlin, A., Hartmann, M., Heintz, D., Hartmann, M.-A., Mutterer, J., Rodríguez-Concepción, M., Boronat, A., Van Dorsselaer, A., Rohmer, M., et al. (2009). The plastidial *2C*-methyl-*D*-erythritol 4-phosphate pathway provides the isoprenyl moiety for protein geranylgeranylation in tobacco BY-2 cells. Plant Cell. **21**, 285–300.

Gershenzon, J., and Croteau, R. (1993). Terpenoid biosynthesis: the basic pathway and formation of monoterpenes, sesquiterpenes, and diterpenes. *In* Lipid Metabolism in Plants, **Moore, T.C.J.**, ed. (Boca Raton, FL: CRC Press), pp. 339–388.

Guirimand, G., Guihur, A., Phillips, M.A., Oudin, A., Glévarec, G., Melin, C., Papon, N., Clastre, M., St-Pierre, B., Rodríguez-Concepción, M., et al. (2012). A single gene encodes isopentenyl diphosphate isomerase isoforms targeted to plastids, mitochondria and peroxisomes in *Catharanthus roseus*. Plant Mol. Biol. **79**, 443–459.

Gupta, M.M., Singh, D.V., Tripathi, A.K., Pandey, R., Verma, R.K., Singh, A.K., Shasany, A.K., and Khanuja, S.P.S. (2005). Simultaneous determination of vincristine, vinblastine, catharanthine and vindoline in leaves of *Catharanthus roseus* by high-performance liquid chromatography. J. Chromatgr. Sci. **43**, 450–453.

Hedhili, S., Courdavault, V., Giglioli-Guivarc'h, N., and Gantet, P. (2007). Regulation of the terpene moiety biosynthesis of *Catharanthus roseus* terpene indole alkaloids. Phytochem. Rev. **6**, 341–351.

Hemmerlin, A., Harwood, J.L., and Bach, T.J. (2012). A raison d'être for two distinct pathways in the early steps of plant isoprenoid biosynthesis? Prog. Lipid Res. **51**, 95–148.

Hsiao, Y.Y., Jeng, M.F., Tsai, W.C., Chuang, Y.C., Li, C.Y., Wu, T.S., Kuoh, C.S., Chen, W.H., and Chen, H.H. (2008). A novel homodimeric geranyl diphosphate synthase from the orchid *Phalaenopsis bellina* lacking a $DD(X)_{2-4}$ motif. Plant J. **55**, 719–733.

Hsieh, F.L., Chang, T.H., Ko, T.P., and Wang, A.H. (2011). Structure and mechanism of an *Arabidopsis* medium/long-chain-length prenyl pyrophosphate synthase. Plant Physiol. **155**, 1079–1090.

Kainou, T., Kawamura, K., Tanaka, K., Matsuda, H., and Kawamukai, M. (1999). Identification of the GGPS1 genes encoding geranylgeranyl diphosphate synthases from mouse and human. Biochim. Biophys. Acta. **1437**, 333–340.

Koyama, T., Tajima, M., Sano, H., Doi, T., Koike-Takeshita, A., Obata, S., Nishino, T., and Ogura, K. (1996). Identification of significant residues in the substrate binding site of *Bacillus stearothermophilus* farnesyl diphosphate synthase. Biochemistry. **35**, 9533–9538.

Lange, B.M., and Ghassemian, M. (2003). Genome organization in *Arabidopsis thaliana*: a survey for genes involved in isoprenoid and chlorophyll metabolism. Plant Mol. Biol. **51**, 925–948.

Liang, P.H., Ko, T.P., and Wang, A.H. (2002). Structure, mechanism and function of prenyltransferases. Eur. J. Biochem. **269**, 3339–3354.

Liscombe, D.K., and O'Connor, S.E. (2011). A virus-induced gene silencing approach to understanding alkaloid metabolism in *Catharanthus roseus*. Phytochemistry. **72**, 1969–1977.

Liu, D.H., Jin, H.B., Chen, Y.H., Cui, L.J., Ren, W.W., Gong, Y.F., and Tang, K.X. (2007). Terpenoid indole alkaloids biosynthesis and metabolic engineering in *Catharanthus roseus*. J. Integr. Plant Biol. **49**, 961–974.

Long, M.C., Nagegowda, D.A., Kaminaga, Y., Ho, K.K., Kish, C.M., Schnepp, J., Sherman, D., Weiner, H., Rhodes, D., and Dudareva, N. (2009). Involvement of snapdragon benzaldehyde dehydrogenase in benzoic acid biosynthesis. Plant J. **59**, 256–265.

Martin, D., Tholl, D., Gershenzon, J., and Bohlmann, J. (2002). Methyl jasmonate induces traumatic resin ducts, terpenoid resin biosynthesis, and terpenoid accumulation in developing xylem of Norway spruce stems. Plant Physiol. **129**, 1003–1018.

Menke, F.L.H., Champion, A., Kijne, J.W., and Memelink, J. (1999). A novel jasmonate- and elicitor-responsive element in the periwinkle secondary metabolite biosynthetic gene Str interacts with a jasmonate- and elicitor-inducible AP2-domain transcription factor, ORCA2. EMBO J. **18**, 4455–4463.

Nagegowda, D.A. (2010). Plant volatile terpenoid metabolism: biosynthetic genes, transcriptional regulation and subcellular compartmentation. FEBS Lett. **584**, 2965–2973.

Nagegowda, D.A., Gutensohn, M., Wilkerson, C.G., and Dudareva, N. (2008). Two nearly identical terpene synthases catalyze the formation of nerolidol and linalool in snapdragon flowers. Plant J. **55**, 224–239.

Ogura, K., and Koyama, T. (1998). Enzymatic aspects of isoprenoid chain elongation. Chem. Rev. **98**, 1263–1276.

Okada, K., Saito, T., Nakagawa, T., Kawamukai, M., and Kamiya, Y. (2000). Five geranylgeranyl diphosphate synthases expressed in different organs are localized into three subcellular compartments in *Arabidopsis*. Plant Physiol. **122**, 1045–1056.

Orlova, I., Marshall-Colón, A., Schnepp, J., Wood, B., Varbanova, M., Fridman, E., Blakeslee, J.J., Peer, W.A., Murphy, A.S., Rhodes, D., et al. (2006). Reduction of benzenoid synthesis in petunia flowers reveals multiple pathways to benzoic acid and enhancement in auxin transport. Plant Cell. **18**, 3458–3475.

Orlova, I., Nagegowda, D.A., Kish, C.M., Gutensohn, M., Maeda, H., Varbanova, M., Fridman, E., Yamaguchi, S., Hanada, A., Kamiya, Y., et al. (2009). The small subunit of snapdragon geranyl diphosphate synthase modifies the chain length specificity of tobacco geranylgeranyl diphosphate synthase in planta. Plant Cell. **21**, 4002–4017.

Oudin, A., Mahroug, S., Courdavault, V., Hervouet, N., Zelwer, C., Rodriguez-Concepcion, M., St-Pierre, B., and Burlat, V. (2007). Spatial distribution and hormonal regulation of gene products from methyl erythritol phosphate and monoterpene-secoiridoid pathways in *Catharanthus roseus*. Plant Mol. Biol. **65**, 13–30.

Pateraki, I., and Kanellis, A.K. (2008). Isolation and functional analysis of two *Cistus creticus* cDNAs encoding geranylgeranyl diphosphate synthase. Phytochemistry. **69**, 1641–1652.

Rijhwani, S.K., and Shanks, J.V. (1998). Effect of elicitor dosage and exposure time on biosynthesis of indole alkaloids by *Catharanthus roseus* hairy root cultures. Biotechnol. Prog. **14**, 442–449.

Rischer, H., Orešič, M., Seppänen-Laakso, T., Katajamaa, M., Freya, L., Ardiles-Diaz, W., Van Montagu, M.C.E., Inzé, D., Oksman-Caldentey, K.M., and Goossens, A. (2006). Gene-to-metabolite networks for terpenoid indole alkaloid biosynthesis in *Catharanthus roseus* cells. Proc. Natl Acad. Sci. U S A. **103**, 5614–5619.

Roepke, J., Salim, V., Wu, M., Thamm, A.M.K., Murata, J., Ploss, K., Boland, W., and De Luca, V. (2010). Vinca drug components accumulate exclusively in leaf exudates of Madagascar periwinkle. Proc. Natl Acad. Sci. U S A. **107**, 15287–15292.

Schmidt, A., and Gershenzon, J. (2007). Cloning and characterization of isoprenyl diphosphate synthases with farnesyl diphosphate and geranylgeranyl diphosphate synthase activity from Norway spruce (*Picea abies*) and their relation to induced oleoresin formation. Phytochemistry. **68**, 2649–2659.

Schmidt, A., and Gershenzon, J. (2008). Cloning and characterization of two different types of geranyl diphosphate synthases from Norway spruce (*Picea abies*). Phytochemistry. **69**, 49–57.

Schmidt, A., Wachtler, B., Temp, U., Krekling, T., Seguin, A., and Gershenzon, J. (2010). A bifunctional geranyl and geranylgeranyl diphosphate synthase is involved in terpene oleoresin formation in *Picea abies*. Plant Physiol. **152**, 639–655.

Sheen, J. (2002). A transient expression assay using *Arabidopsis* mesophyll protoplasts. Available online at http://genetics.mgh.harvard.edu/sheenweb/.

Simkin, A.J., Miettinen, K., Claudel, P., Burlat, V., Guirimand, G., Courdavault, V., Papon, N., Meyer, S., Godet, S., St-Pierre, B., et al. (2012). Characterization of the plastidial geraniol synthase from Madagascar periwinkle which initiates the monoterpenoid branch of the alkaloid pathway in internal phloem associated parenchyma. Phytochemistry. **85**, 36–43.

Singh, D.V., Maithy, A., Verma, R.K., Gupta, M.M., and Kumar, S. (2000). Simultaneous determination of *Catharanthus* alkaloids using reversed phase high performance liquid chromatography. J. Liq. Chromatogr. **23**, 601–607.

St-Pierre, B., Vázquez-Flota, F.A., and De Luca, V. (1999). Multicellular compartmentation of *Catharanthus roseus* alkaloid biosynthesis predicts intercellular translocation of a pathway intermediate. Plant Cell. **11**, 887–900.

Takaya, A., Zhanga, W., Asawatreratanakul, K., Wititsuwannakul, D., Wititsuwannakul, R., Takahashi, S., and Koyama, T. (2003). Cloning, expression and characterization of a functional cDNA clone encoding geranylgeranyl diphosphate synthase of *Hevea brasiliensis*. Biochim. Biophys. Acta. **1625**, 214–220.

Tamura, K., Dudley, J., Nei, M., and Kumar, S. (2007). MEGA4: Molecular Evolutionary Genetics Analysis (MEGA) software version 4.0. Mol. Biol. Evol. **24**, 1596–1599.

Thabet, I., Guirimand, G., Courdavault, V., Papon, N., Godet, S., Dutilleul, C., Bouzid, S., Giglioli-Guivarc'h, N., Clastre, M., and Simkin, A.J. (2011). The subcellular localization of periwinkle farnesyl diphosphate synthase provides insight into the role of peroxisome in isoprenoid biosynthesis. J. Plant Physiol. **168**, 2110–2116.

Thabet, I., Guirimand, G., Guihur, A., Lanoue, A., Courdavault, V., Papon, N., Bouzid, S., Giglioli-Guivarc'h, N., Simkin, A.J., and Clastre, M. (2012). Characterization and subcellular localization of geranylgeranyl diphosphate synthase from *Catharanthus roseus*. Mol. Biol. Rep. **39**, 3235–3243.

Tholl, D., Kish, C.M., Orlova, I., Sherman, D., Gershenzon, J., Pichersky, E., and Dudareva, N. (2004). Formation of monoterpenes in *Antirrhinum majus* and *Clarkia breweri* flowers involves heterodimeric geranyl diphosphate synthases. Plant Cell. **16**, 977–992.

Tsai, W.C., and Chen, H.H. (2006). The orchid MADS-box genes controlling floral morphogenesis. Sci. World J. **6**, 1933–1944.

Turner, G.W., and Croteau, R. (2004). Organization of monoterpene biosynthesis in *Mentha*: immunocytochemical localizations of geranyl diphosphate synthase, limonene-6-hydroxylase, isopiperitenol dehydrogenase, and pulegone reductase. Plant Physiol. **136**, 4215–4227.

van der Fits, L., and Memelink, J. (2001). The jasmonate-inducible AP2/ERF-domain transcription factor ORCA3 activates gene expression via interaction with a jasmonate responsive promoter element. Plant J. **25**, 43–53.

van der Heijden, R., Jacobs, D.I., Snoeijer, W., Hallard, D., and Verpoorte, R. (2004). The *Catharanthus* alkaloids: pharmacognosy et biotechnology. Curr. Med. Chem. **11**, 1241–1253.

van Schie, C.C.N., Ament, K., Schmidt, A., Lange, T., Haring, M.A., and Schuurink, R.C. (2007). Geranyl diphosphate synthase is required for biosynthesis of gibberellins. Plant J. **52**, 752–762.

Vázquez-Flota, F.A., and De Luca, V. (1998). Developmental and light regulation of desacetoxyvindoline 4-hydroxylase in *Catharanthus roseus* (L.) G. Don: evidence of a multilevel regulatory mechanism. Plant Physiol. **117**, 1351–1361.

Veau, B., Courtois, M., Oudin, A., Chénieux, J.C., Rideau, M., and Clastre, M. (2000). Cloning and expression of cDNAs encoding two enzymes of the MEP pathway in *Catharanthus roseus*. Biochim. Biophys. Acta. **1517**, 159–163.

Wang, G., and Dixon, R.A. (2009). Heterodimeric geranyl(geranyl) diphosphate synthase from hop (*Humulus lupulus*) and the evolution of monoterpene biosynthesis. Proc. Natl Acad. Sci. U S A. **106**, 9914–9919.

Wang, K., and Ohnuma, S. (2000). Isoprenyl diphosphate synthases. Biochim. Biophys. Acta. **1529**, 33–48.

Wang, Y., Miao, Z., and Tang, K. (2010). Molecular cloning and functional expression analysis of a new gene encoding geranylgeranyl diphosphate synthase from hazel (*Corylus avellana* L. Gasaway). Mol. Biol. Rep. **37**, 3439–3444.

Wei, S. (2010). Methyl jasmonic acid induced expression pattern of terpenoid indole alkaloid pathway genes in *Catharanthus roseus* seedlings. Plant Growth Regul. **61**, 243–251.

SUMMARY

This work suggests that, in *Catharanthus roseus*, the inactive small subunit of heteromeric GPP synthase (GPPS) interacts with bifunctional G(G)PPS and redirects the metabolic flux, thus acting as primary regulator of monoterpene indole alkaloid biosynthesis, whereas homomeric GPPS could be involved in ubiquinone formation.